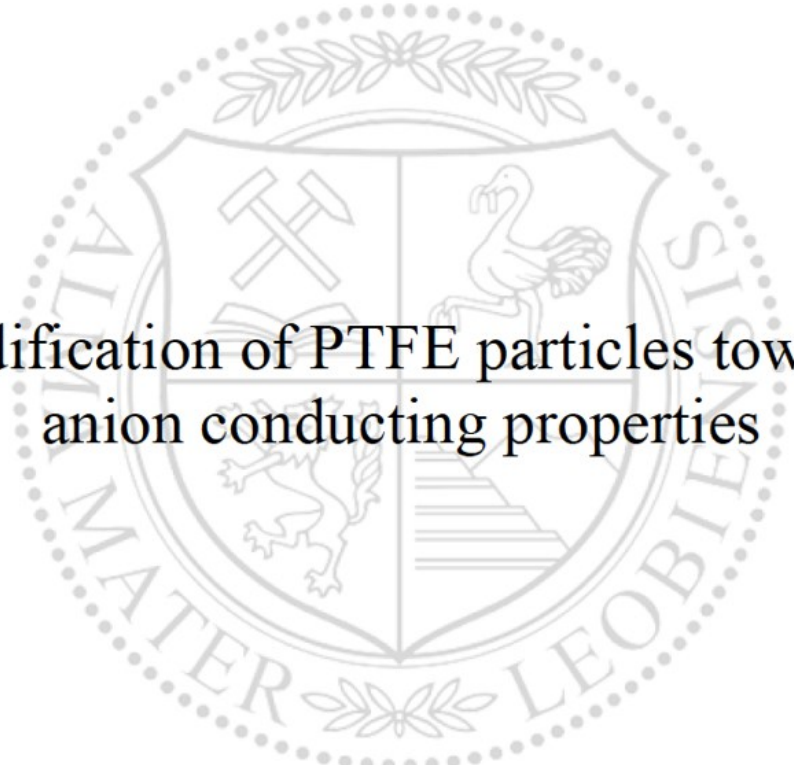




Chair of Chemistry of Polymeric Materials

Master's Thesis



Modification of PTFE particles towards
anion conducting properties

Benjamin Sydor, BSc

October 2024



Head of Institute: Univ.-Prof. Dipl.-Ing. Dr.techn. Thomas Griebner

Leoben, October 2024



MONTANUNIVERSITÄT LEOBEN

www.unileoben.ac.at

EIDESSTÄTLICHE ERKLÄRUNG

Ich erkläre an Eides statt, dass ich diese Arbeit selbstständig verfasst, andere als die angegebenen Quellen und Hilfsmittel nicht benutzt, den Einsatz von generativen Methoden und Modellen der künstlichen Intelligenz vollständig und wahrheitsgetreu ausgewiesen habe, und mich auch sonst keiner unerlaubten Hilfsmittel bedient habe.

Ich erkläre, dass ich den Satzungsteil „Gute wissenschaftliche Praxis“ der Montanuniversität Leoben gelesen, verstanden und befolgt habe.

Weiters erkläre ich, dass die elektronische und gedruckte Version der eingereichten wissenschaftlichen Abschlussarbeit formal und inhaltlich identisch sind.

Datum 20.10.2024

Unterschrift Verfasser/in
Benjamin Sydor

Acknowledgements

I would like to express my sincerest gratitude to all those who have supported me during my master's programme and thesis.

Firstly, I would like to express my gratitude to Prof. Wolfgang Kern for giving me the opportunity to write my master's thesis at the Chair of Chemistry of Polymeric Materials. Though Prof. Wolfgang Kern unfortunately is no longer with us, his expertise and ongoing support have made an important contribution to my thesis and my personal development as a polymer engineer.

Hereby, I would also like to thank to Prof. Thomas Grießer for his invaluable assistance, which enables me to complete my master's programme following the passing of Prof. Wolfgang Kern.

Furthermore, I would like to thank my supervisor Dr. mont. Christine Bandl for her guidance and immense support during my work in her working group and the course of my master's thesis. Her encouragement and patient commitment to provide detailed explanations have been very valuable to me many times during my master's programme.

I would also like to thank all my dear colleagues at the Chair of Chemistry of Polymeric Materials for the ongoing support and the countless joyful hours full of motivation during our everyday laboratory work.

I would also like to extend my gratitude to the team of the HyCentA Research GmbH for their cooperation and assistance during the project.

Furthermore, I would like to thank the company Diener electronic GmbH + Co. KG for their consulting, technical support and for providing the resources to treat our samples with NH_3 plasma at their company site.

Finally, I would like to thank my parents for making this study programme possible for me. Without their support, I would never have been able to successfully complete my studies. Furthermore, I would like to express my deepest gratitude to my girlfriend Julia for her unwavering patience and for continuously lifting my spirits during challenging periods. The love and encouragement of my family and friends have made my work possible!

Abstract

The objective of this master's thesis was to functionalise polytetrafluoroethylene (PTFE) particles towards anion conducting properties for the use as a binder material in anion exchange membrane (AEM) water electrolysis cells. The functionalisation of PTFE particle surfaces was divided into three process stages: the activation of the surface, the introduction of amino (NH_2) groups to the activated surface and the quaternisation of the NH_2 groups. After each individual process stage the PTFE particles were analysed with an X-ray photoelectron spectroscope (XPS) to determine the surface composition. Within the scope of this thesis, the activation of the PTFE particle surface via hydrogen (H_2) plasma and the introduction of NH_2 groups via silanisation or ammonia (NH_3) plasma have proven to be successful, whereas the quaternization requires further investigation. The findings presented within this thesis provide a crucial foundation for further research into the functionalisation of PTFE particles to achieve the required properties for AEM water electrolysis cells.

Kurzfassung

Ziel dieser Masterarbeit war die Funktionalisierung von Polytetrafluorethylen (PTFE)-Partikeln zur Einführung von anionenleitenden Gruppen für den Einsatz als Bindermaterial in Anionenaustauschmembran (AEM)-Wasserelektrolysezellen. Die Funktionalisierung der Oberfläche von PTFE-Partikeln wurde hierbei in drei Prozessschritte unterteilt: die Aktivierung der Partikeloberfläche, die Einführung von Aminogruppen (-NH₂) an der aktivierten Oberfläche und die Quaternisierung dieser NH₂-Gruppen. Nach jedem einzelnen Prozessschritt wurden die PTFE-Partikel mit einem Röntgenphotoelektronenspektroskop (XPS) analysiert, um die Oberflächenzusammensetzung zu bestimmen. Im Rahmen dieser Arbeit haben sich die Aktivierung der PTFE-Partikeloberfläche mittels Wasserstoffplasmas (H₂-Plasma) sowie die Oberflächenaktivierung und das Einbringen von NH₂-Gruppen mittels Ammoniakplasmas (NH₃-Plasma) als erfolgreich erwiesen. Diese Ergebnisse bilden eine wichtige Grundlage für weitere Forschungen zur Funktionalisierung von PTFE-Partikeln, um die erforderlichen Eigenschaften für AEM-Wasserelektrolysezellen zu erreichen.

List of abbreviations

Abbreviation	Meaning
AWE	Alkaline water electrolysis
PEM	Proton exchange membrane water electrolysis
SOE	Solid oxide water electrolysis
AEM	Anion exchange membrane water electrolysis
HER	Hydrogen evolution reaction
OER	Oxygen evolution reaction
PTFE	Polytetrafluoroethylene
TFE	Tetrafluoroethylene
APTES	(3-Aminopropyl)triethoxysilane
DMAEA	2-Dimethylaminoethyl acrylate
DMVA	N,N-Dimethyl-4-vinylaniline
QAC	Quaternary ammonium compound
XPS	X-ray photoelectron spectroscopy

Table of contents

Acknowledgements	I
Abstract	III
Kurzfassung	IV
List of abbreviations	V
Table of contents	VII
1 Introduction	1
2 Theoretical background	1
2.1 Green energy	1
2.2 Hydrogen production by water electrolysis	2
Working principle of water electrolysis	2
Alkaline water electrolysis (AWE)	5
Proton exchange membrane water electrolysis (PEM)	7
Solid oxide water electrolysis (SOE)	9
Anion exchange membrane water electrolysis (AEM).....	10
Conclusion and comparison of water electrolysis technologies	12
2.3 Polytetrafluoroethylene (PTFE)	14
PTFE production	14
PTFE characteristics	15
2.4 Plasma treatment of surfaces	16
2.5 Quaternary ammonium compounds	19
QAC characteristics and applications	19
QAC production	20
2.6 Characterisation methods	22
X-ray photoelectron spectroscopy (XPS).....	22
3 Experimental	26
3.1 Chemicals, materials and equipment	26
3.2 Sample preparation	30

Activation via O ₂ , Ar or H ₂ plasma and introduction of amino groups via APTES30	
Activation via Ar plasma and introduction of amino groups via “grafting-from” reaction	32
Activation and introduction of amino groups via NH ₃ plasma	33
3.3 Characterisation.....	34
X-ray photoelectron spectroscope (XPS).....	34
4 Results and discussion	35
Surface modification via plasma treatment and subsequent silanisation with APTES	35
Surface modification via Ar plasma and subsequent “grafting-from” reactions .	46
Surface modification via NH ₃ plasma	49
Quaternisation.....	51
5 Conclusion and outlook	54
6 List of figures	56
7 List of tables.....	58
8 Bibliography.....	59
9 Appendix.....	64
9.1 AI declaration	64

1 Introduction

Since polytetrafluoroethylene (PTFE) is one of the most chemically inert polymers characterised by its hydrophobicity and poor adhesion [1], many efforts have been made to suitably functionalise the surface of PTFE particles for their use as a binder in anion exchange membrane water electrolysis cells. Based on the preliminary work in the bachelor thesis "Functionalisation and characterisation of PTFE films towards increased surface polarity and ion conductivity" of my dear colleague Sebastian Ernst, BSc, the aim of this master thesis is to transfer the developed modification processes from PTFE films to PTFE particles.

2 Theoretical background

2.1 Green energy

With the growing aspiration to replace fossil and nuclear energy sources to reduce the environmental footprint, various renewable energy sources like wind power, hydropower and solar photovoltaic energy have been developed, optimised and integrated into the general electricity grid over the course of the last century [2]. These renewable technologies can be used to produce green energy, which can be defined as energy from sources with minimal or zero environmental impact. Given the finite nature of the Earth's fossil fuel reserves, green energy represents a promising opportunity for enhancing energy security [3]. Hereby, energy security is defined as the constant availability and affordability of energy sources [4]. Furthermore, green energy reduces environmental pollution, energy-related illnesses or fatalities and political conflicts between energy-producing and energy-purchasing countries. The selection of an appropriate green energy source strongly depends on local conditions leading to a decentralisation [3]. To incorporate renewable power into the electric system efficiently and sustainably, many challenges regarding the energy storage and reliability must be overcome. The amount of energy produced by renewable energy sources is underlying heavy fluctuations depending on environmental conditions, such as the weather and daylight. Therefore, a lot of effort is being put into the development of efficient energy storages to establish a constant power supply by retaining energy surpluses and compensating temporary supply deficits [2].

2.2 Hydrogen production by water electrolysis

Recent developments offer hydrogen technology as a suitable method to overcome these challenges described in section 2.1. Hydrogen has multiple potential applications, such as being an essential agent for the production of many chemicals and the processing of crude oil [5]. Furthermore, hydrogen is considered a fuel and is approximately three times more energetic than gasoline [2]. Therefore, it can also be used as an alternative to fossil fuels for powering zero-emission vehicles [6]. Due to its storage ability, hydrogen can be used for energy storage and later re-electrification in fuel cells to overcome energy security problems of green energy sources [7]. Hydrogen is the most abundant element in the universe, although it does not occur in its pure state. It can be conventionally produced by steam reforming and partial oxidation of hydrocarbons in fossil fuels or biomass and by thermal decomposition of water. While using fossil fuels for the hydrogen production is not a sustainable solution, the thermal decomposition of water leads to problems with corrosion and the demand for heat sources to achieve temperatures over 850 °C. Therefore, a very promising alternative without the emission of pollutant gases and the use of non-renewable resources is the production of hydrogen by water electrolysis [2].

Working principle of water electrolysis

In the electrolysis process electrical energy is used to initiate and sustain a chemical dissociation and ion generating reaction in a so-called electrolytic cell [8]. Generally, an electrolytic cell mainly contains two separate electrodes (anode and cathode), an electrolyte, a metallic path and a DC power source [7], [9]. To avoid the recombination of the generated ions a diaphragm or separator can be placed between the electrodes [2]. In an electrolytic cell two different principles of conducting electricity can be found. The conductivity of metals is caused by the movement of electrons and therefore called metallic or electronic conductivity. In contrast, the conductivity of an electrolyte solution is based on ion movement and therefore called electrolytic or ionic conductivity [8], [10]. As a result, the diaphragm should exhibit a high ionic conductivity while its electrical resistance should prevent short-circuiting of the electrodes [2]. The electrodes are made of two dissimilar metals that must be corrosion-resistant and exhibiting a good electronic conductivity and structural integrity [2], [9]. Both electrodes are immersed in the electrolyte, which is an ionically

conducting solid material or liquid solution that must not react with the electrodes, while being externally connected with a DC voltage source by the metallic path [2], [9], [11]. The fundamental design of a water electrolysis cell containing these components is shown in the following Figure 1 [12].

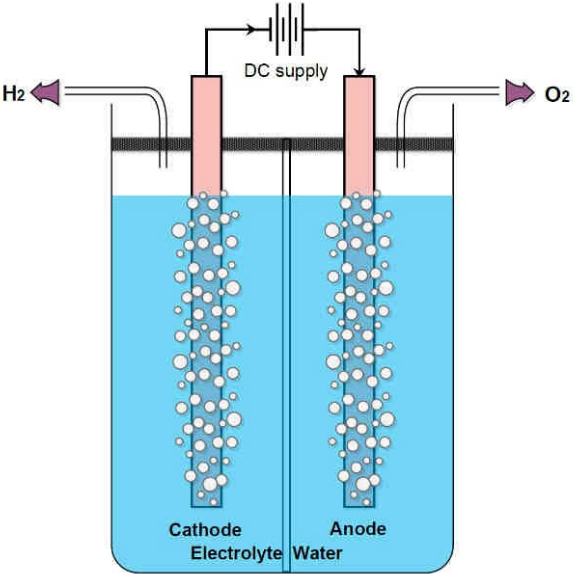


Figure 1: Fundamental design of a water electrolysis cell [12].

Figure 2 shows two different water electrolysis cell designs: the conventional cell and the zero-gap cell [13]. While the conventional cell is characterised by a gap between the electrodes and the separator, the electrodes in the zero-gap cell are porous and pressed directly onto the separator [7].

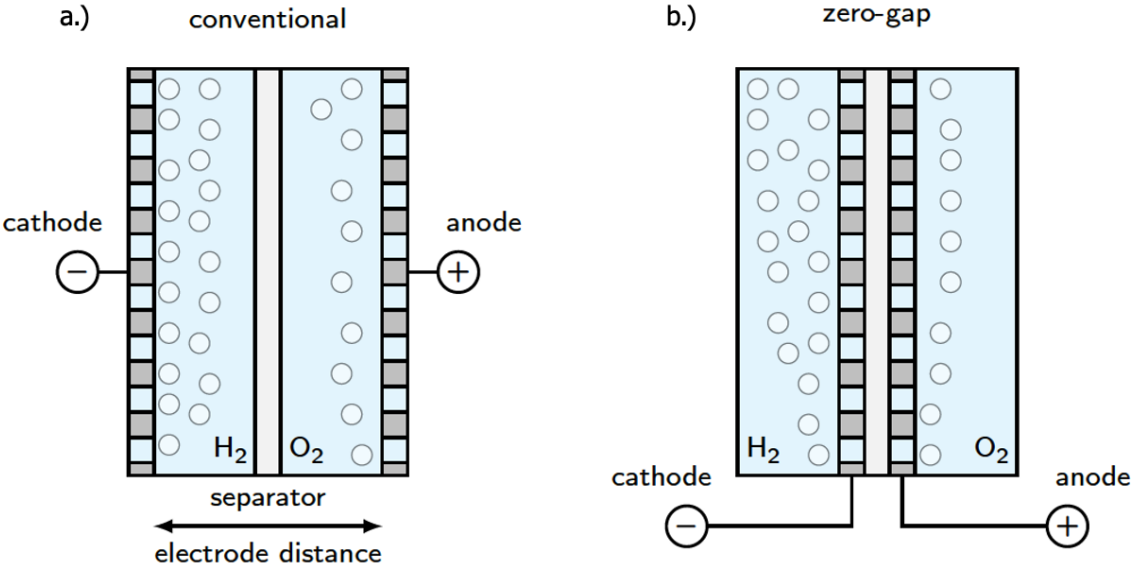
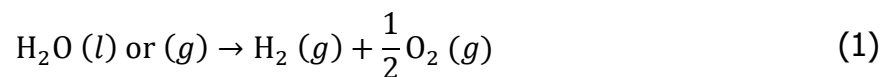


Figure 2: Water electrolysis cell designs: a.) conventional and b.) zero-gap [13].

To meet the respective requirements regarding the hydrogen production rate usually multiple cells are connected forming a module called the cell stack. If the cells are connected in parallel each electrode has one single polarity and the configuration is called monopolar. In case of a series configuration each electrode – except for the first and last electrode – has two polarities and the module is therefore called bipolar. Bipolar modules are more space saving and can reach the same hydrogen production rate with a lower current than monopolar modules. Therefore, series connection of cells within a bipolar module has proven to be more suitable for hydrogen production and is nowadays used by most electrolyser manufacturers [2].

In order to perform the electrolysis of water a DC voltage is applied to two electrodes submerged in liquid water or water vapor leading to the dissociation and generation of hydrogen and oxygen in their gaseous states according to the following overall reaction equation (1) [2], [7].



This overall reaction (1) is the sum of a reduction half-reaction and an oxidation half-reaction [7]. The anode is defined as the electrode at which the oxidation half-reaction occurs, leading to an electron release and therefore a positive polarisation. Due to the voltage source, the released electrons follow the metallic path to the other electrode called the cathode causing its negative polarisation and electron consumption by the reduction half-reaction [8], [9]. Therefore, in the resulting electric field between the electrodes, the positively charged ions known as cations migrate to the cathode while the negatively charged ions called anions move towards the anode due to electrolytic conduction. At the cathode, the H^+ cations absorb electrons and are reduced to hydrogen. Meanwhile at the anode, the OH^- anions release their electrons and are oxidised to oxygen [8]. As a result, hydrogen/water and oxygen/water mixtures can be obtained at specific exhausts on either side of the diaphragm [7]. In order for hydrogen to be stored, it must undergo a compression process by either performing the electrolysis under pressure or by a mechanical compression following the electrolysis. Furthermore, the amount of water vapor in the gases obtained from an electrolyser under pressure is much lower in comparison to an electrolyser operating

at atmospheric pressure reducing the cost of subsequent drying processes [14]. The generated hydrogen and oxygen subsequently undergo various treatments such as cooling and purification before they can be stored. In many cases the produced and processed oxygen is then released into the atmosphere [2].

Although its many advantages over the conventional ways of hydrogen production, the production capacities needed by the economy are yet to be realised. Since its beginnings over a hundred years ago intensive research and work has been put into the development of a large-scale renewable hydrogen production leading to three main types of commercially available water electrolysis technologies: the alkaline water electrolysis (AWE), the proton exchange membrane (PEM) water electrolysis, and the solid oxide electrolysis (SOE) [2], [7]. Furthermore, a new promising technology called anion exchange membrane (AEM) water electrolysis is being developed to overcome the disadvantages of the established technologies [15].

Alkaline water electrolysis (AWE)

Historically, AWE is the oldest water electrolysis technology and has become a well-established and reliable method for hydrogen production. An AWE cell usually contains two porous electrodes separated by a gas-tight diaphragm and immersed in an alkaline liquid electrolyte [2]. This assembly can either be a gap or zero-gap cell configuration, although the zero-gap design is more efficient reaching higher current density values [14]. The alkaline electrolyte is usually an aqueous solution with 25 – 30 wt.% KOH to optimise the ionic conductivity. In the past, the diaphragms were made of asbestos which proved to be unsuitable due to their toxicity and gas permeability [7]. Nowadays, ion exchange inorganic membranes, such as ZrO₂ on a polysulfone matrix (ZIRFON®), are most widely used instead [2]. The electrodes are usually steel grids, which in some applications are additionally coated with a porous nickel layer. The following Figure 3 shows the structure of an AWE cell [16].

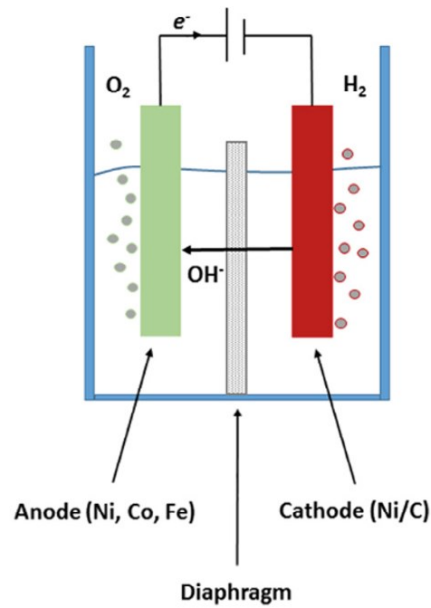
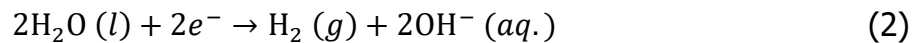


Figure 3: AWE cell structure [16].

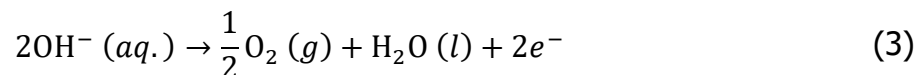
Most alkaline water electrolyzers contain several hundred of these cells connected in series [14]. In an elementary cell, water is reduced at the cathode according to the following cathode half reaction equation (2) yielding hydrogen gas and hydroxide anions [2], [7].

Cathode half reaction:



The external power supply generates an electric field allowing the hydroxide anions to migrate through the separator to the anode. At the surface of the anode, the hydroxide anions recombine generating oxygen and water according to the following anode half reaction equation (3) [2], [7].

Anode half reaction:



Although there are certain alkaline water electrolyser prototypes working at much higher temperatures and pressures, the electrolysis is usually carried out in a temperature range from 60 °C to 90 °C and at pressures up to 30 bar [2], [17]. As water is consumed in the reaction, it must be supplied to the cell continuously to

maintain the reaction and the optimal concentration of the electrolyte. Although water can be used without prior purification steps, the hydrogen produced contains impurities of oxygen and water vapor with alkali [14]. To improve the purity level and therefore the quality of the produced hydrogen, either the water fed to the cell has to be significantly pure or further hydrogen purification steps are necessary [2], [14]. AWE cells exhibit a low maximum current density ($< 0.5 \text{ A cm}^{-2}$) resulting in lower production rates [5], [17]. Furthermore, while the use of low-cost electrode materials such as nickel alloy-plated steel makes the AWE technology appear economically attractive, the corrosive character of the alkaline electrolytes has proven to be a major challenge [5].

Proton exchange membrane water electrolysis (PEM)

The following Figure 4 shows the general structure of a proton exchange membrane water electrolysis (PEM) cell [18].

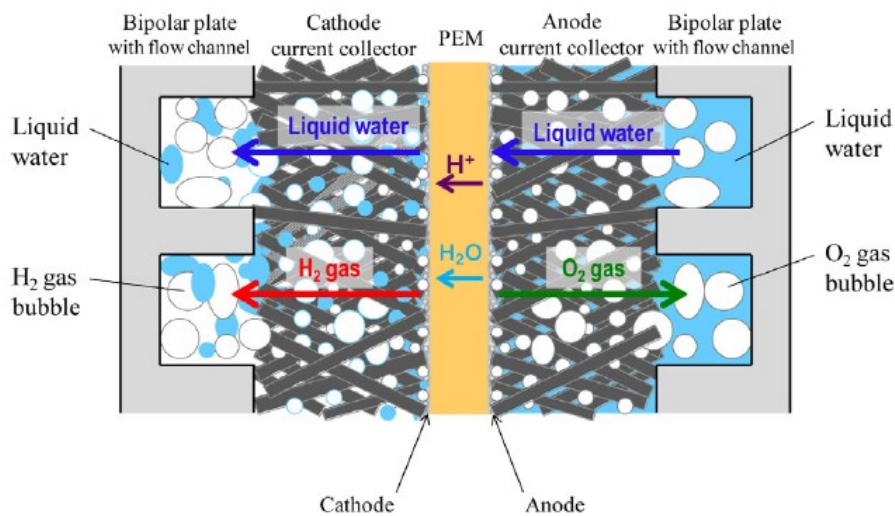
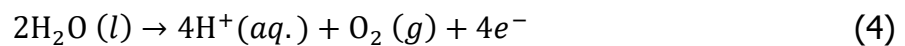


Figure 4: PEM cell structure [18].

In a PEM cell, a perfluorosulfonic acid membrane is used as a solid electrolyte [5]. The membrane is coated on each side with catalytic layers that serve as the electrodes [19]. This catalytic layer is typically composed of noble metals with high price points, such as iridium oxide on the anode side and platinum on the cathode side [5]. Furthermore, polymer solutions called ionomers or binders are added to the catalytic layer leading to a high ionic conductivity, mechanical stability and durability of the structure. The most widely used and investigated ionomer in PEM cells is Nafion[®] by DuPont, but its high price, reduced ion conductivity at temperatures above 100 °C

and possible thermal degradation can limit its suitability [20], [21]. The membrane, in conjunction with the anode and cathode, forms the so-called membrane electrode assembly (MEA) [2]. To complete a PEM cell, current collectors and separator plates are added to the MEA on both sides. The current collectors are typically made of sintered titanium powder and the separator plates are usually made of either titanium, graphite or coated stainless steel [21]. Water is pumped into the cell from the anode side where it flows through channels integrated into the separator plates and diffuses through the porous structure of the current collectors before it reaches the catalytic layer [7], [21]. At the catalytic layer of the anode, water is oxidised producing oxygen, H⁺ cations and electrons according to the reaction equation (4) [2], [16].

Anode half reaction:



The membrane then conducts the H⁺ cations from the anode to the cathode where they are reduced producing hydrogen gas according to the following reaction equation (5) [2], [16].

Cathode half reaction:



PEM cells usually operate in a temperature range from 50 °C to 90 °C and at pressures up to 350 bar [7], [17]. Hereby, the high operating pressure promotes the storage of the hydrogen produced. PEM offers a high current density (~ 2 A cm⁻²) leading to high production rates, but the corrosive character of the polymer membranes acidic interface leads to short lifetimes and requires expensive platinum group metal (PGM)-based electrocatalysts as well as titanium current collectors and separator plates [2], [5], [17]. The platinum group metals consist of the six adjacent metallic elements platinum, iridium, palladium, osmium, rhodium and ruthenium [22]. Although being commercially available, the PEM technology has only been used for special applications so far due to the expensive cell components [5].

Solid oxide water electrolysis (SOE)

Solid oxide water electrolysis (SOE) cells, as shown in the following Figure 5, allow high temperature steam electrolysis at pressures from 1 to 5 bar due to the possible high cell operating temperatures between 700 and 1000 °C [7], [16].

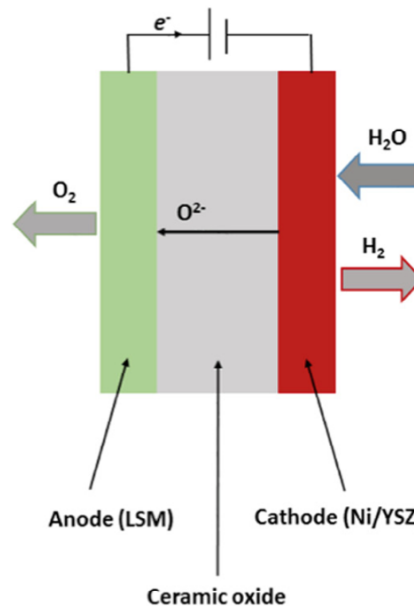
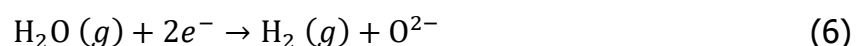


Figure 5: SOE cell structure [16].

The electrodes have a porous structure and are usually made of ceramic and metal composite materials, also called cermets. While the cathode is usually made of nickel and yttria-stabilised zirconia, the anode usually consists of yttria-stabilised zirconia and metals with perovskite structure such as lanthanum, ferrites or cobaltites partially substituted with strontium [2]. The electrolyte is a gas-tight thin film of yttria-stabilised zirconia and the bipolar plates are made of stainless steel [14], [23]. Steam is supplied at the cathode, which leads to the reduction of water producing hydrogen and oxide anions according to the following reaction equation (6) [2].

Cathode half reaction:



The oxide anions move across the solid electrolyte to the anode where they combine producing oxygen according to equation (7) [2].

Anode half reaction:



SOE cells exhibit a high efficiency because the high operating temperatures increase the reaction rate. However, the high temperatures also have a detrimental effect and are a major challenge regarding the thermal stability of the cell components. Furthermore, the reaction product at the cathode is a mixture of hydrogen and steam requiring further purification processes drastically increasing the costs of SOE systems [2]. Therefore, SOE is still under development and has been limited to the lab scale so far [2], [7].

Anion exchange membrane water electrolysis (AEM)

In addition to the currently available technologies mentioned above, a rather new technology called anion exchange membrane water electrolysis (AEM) is being developed [15]. The goal of AEM is to combine the advantages of PEM, such as producing pure hydrogen at a high current density ($\sim 2 \text{ A cm}^{-2}$) with the advantages of AWE using inexpensive materials [17]. A single AEM cell consists of two porous metal framework electrode packages, an anion exchange membrane and two bipolar end plates [24]. Each electrode package consists of a porous transport layer (PTL) and a catalytic layer between the electrode and the membrane [5], [17], which is applied by using ion conducting binders. The porous transport layer ensures an efficient water transport towards the cathode catalyst layer with the simultaneous removal of gaseous reaction products and is therefore also called gas diffusion layer (GDL) [15], [17]. The general configuration of an AEM water electrolysis cell is shown in the following Figure 6 [24].

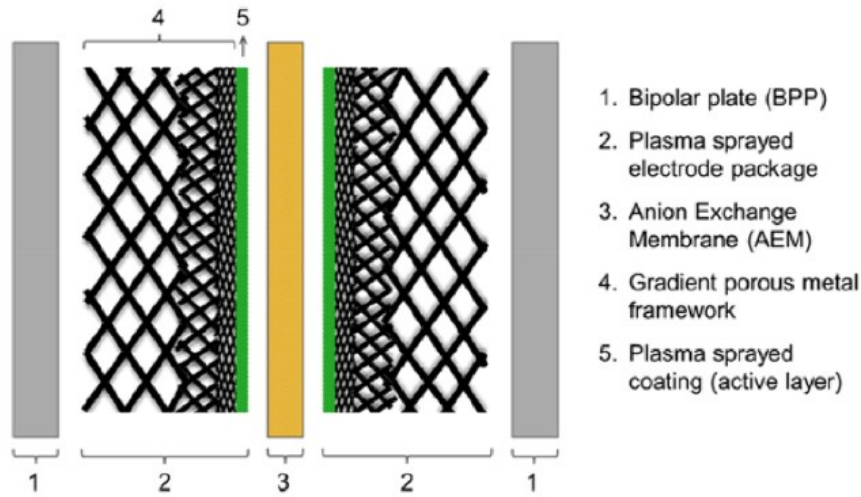
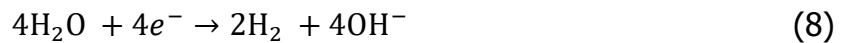


Figure 6: AEM cell structure [24].

The anion exchange membrane and the binder are the most important components of an AEM cell and have so far been manufactured from a polymer backbone with grafted cationic functional groups enabling the required anion exchange [5], [15]. The bipolar plates as shown in Figure 6 are usually made of nickel or stainless steel and are used to separate each cell within a cell stack [15], [17]. Due to their abundance and therefore lower cost, PGM-free materials are used as non-noble metal electrocatalysts to produce the porous electrodes [5], [24]. For the hydrogen evolution reaction (HER) at the cathode, Ni-based and Ni-Mo alloy electrocatalysts have been investigated. Due to their high activity Ni-Mo alloys are the most promising class of HER electrocatalysts. For the oxygen evolution reaction (OER) at the anode, Ni-Fe alloys and Ni- and Cu/Co-mixed spinel-type oxides are likely the most efficient electrocatalysts according to current research. In AEM electrolysis water is fed to the cathode where it is reduced producing hydrogen according to the following HER-reaction equation (8) [5].

Cathode half reaction:



The generated hydroxy anions then migrate through the anion exchange membrane causing the following OER-reaction (9) at the anode producing water and oxygen [5].

Anode half reaction:



In the development of AEM water electrolysis cells, the use of pure water or mild alkaline solutions as an electrolyte has been investigated, but it is still uncertain which electrolyte will prevail in the future. Pure water as an electrolyte is very desirable for reducing equipment costs, but its low ionic conductivity and high ohmic resistance require the application of high voltages decreasing the cell's durability. Mild alkaline solution electrolytes accelerate the ion transfer and therefore result in a higher cell activity, but the long-term stability of the cell components in mild alkaline environment is yet to be investigated [17].

Conclusion and comparison of water electrolysis technologies

Of the four water electrolysis technologies described in this chapter, AWE is the most mature technology and was first developed by J.R. Deiman and A.P. van Trooswijk in 1789 [25]. At the turn of the 20th century, AWE was already widely used in industry [2]. AWE cells use highly concentrated alkaline electrolytes allowing the use of nickel current collectors and noble metal-free electrodes drastically reducing the equipment costs and extending the durability [17]. A disadvantage, however, is the low achievable current density, the additional equipment required for hydrogen purification and low operating pressure, which complicates the hydrogen storage [15], [17]. In addition, AWE cells take time to reach their operating point and react slowly to changes in load, which in turn limits their use for renewable energy sources such as wind power or photovoltaic plants [17]. In 1966, the PEM technology was developed by General Electric and PEM water electrolyzers became commercially available in 1978 [2]. In comparison to AWE, PEM water electrolyzers offer a production of hydrogen with high purity using a pure water feed at high operating pressures also simplifying the hydrogen storage. Furthermore, PEM cells are more suitable for use in combination with intermittent sources of renewable energy. Due to the strongly acidic environment at the polymer membranes interface expensive titanium-based bipolar plates and PGM-based electrocatalysts are required. The high acquisition costs and, in comparison to AWE, lower durability has limited the use of PEM to small-scale applications so far [17]. In comparison to the low-temperature water electrolysis technologies AWE and PEM, SOE operates at high temperatures of 700 °C to 1000 °C causing new challenges concerning the thermal stability of cell components [7], [17]. The SOE technology is still in the research and development stage, but the cell operation at high temperatures

has proven to enhance the hydrogen production and increase the cell efficiency. In the future, the SOE technology could be used in combination with high heat energy sources such as nuclear reactors [2]. In addition, a rather new low-temperature water electrolysis technology called AEM is being developed to compete with the more mature technologies [15]. In comparison to AWE and PEM, PGM-free electrocatalysts and nickel or stainless steel bipolar plates in AEM water electrolysis cells drastically reduce the investment cost [5], [17]. Furthermore, AEM cells operate at a high pressure, which in turn is favourable for the hydrogen storage [15]. The long-term durability of AEM cells is yet to be investigated, but cell components such as the currently available binders have shown limited thermal stability [5], [15]. Therefore, the focus of this work is to develop a thermally more stable binder material based on PTFE particles.

2.3 Polytetrafluoroethylene (PTFE)

PTFE production

Polytetrafluoroethylene (PTFE) was accidentally invented by Roy J. Plunkett in 1938 during his work for the DuPont company [26]. Plunkett named the newly discovered polymer polytetrafluoroethylene which later became the Teflon® trademark by DuPont [27]. The following Figure 7 shows the structural formula of PTFE.

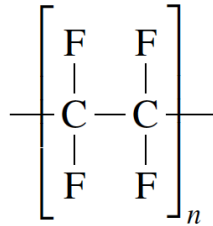


Figure 7: Structural formula of PTFE.

In today's PTFE production, tetrafluoroethylene (TFE) with the semi-structural formula ($\text{CF}_2=\text{CF}_2$) is the basic monomer building block used for further polymerisation [28]. Since TFE is in a gaseous state in standard conditions, high-pressure, stirred-tank, semi-batch reactors are used on an industrial scale for the polymerisation process. Depending on the form of the product, two main types of free-radical polymerisation procedures in aqueous media have evolved for PTFE production [29]. Suspension polymerisation leads to strand-shaped or granular PTFE, while dispersion or emulsion polymerisation produces fine powder PTFE [28], [29]. The mechanism of radical-initiated TFE homopolymerisation is shown in the following Figure 8 [30].

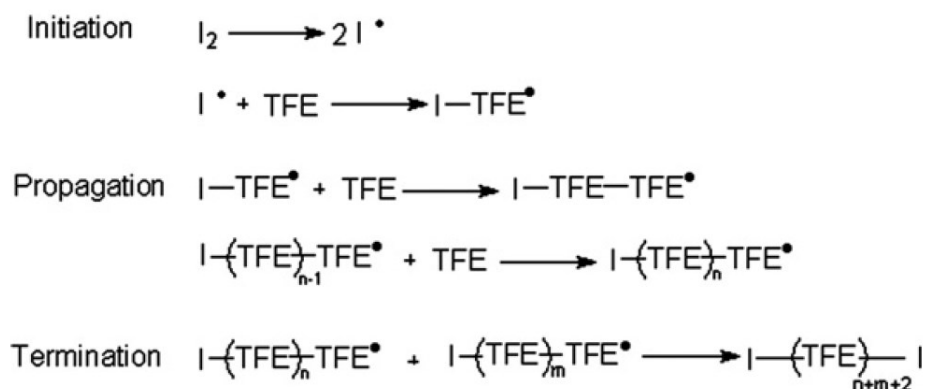


Figure 8: Mechanism of radical-initiated homopolymerisation of [30].

PTFE characteristics

The properties of PTFE are determined by its chemical structure. Given that fluorine possesses the highest electronegativity of all elements in the periodic table, the carbon-fluorine bond (C-F) is polar. The C-F bond is the strongest bond in organic chemistry with a bond energy of approximately 460 kJ/mol [29], [31]. Although the C-F bond itself is polar, PTFE is a non-polar substance due to its completely symmetrical molecular structure. This further makes PTFE a highly hydrophobic material exhibiting poor wettability for all liquids and strong anti-adhesive properties [32]. In terms of stability, PTFE is chemically inert and therefore resistant to all common chemicals, except fluorine and molten alkali metals. Furthermore, PTFE is insoluble in all common solvents and not prone to swelling [29], [32].

PTFE is a semi-crystalline, white solid material consisting of almost completely unbranched polymer chains with a high polymerisation degree. The symmetric molecular structure and large van der Waals radius of the fluorine atoms (0,135 nm in comparison to hydrogen with 0,12 nm) lead to a complete shielding of the carbon backbone. Furthermore, due to the steric hindrance caused by the fluorine atoms, the chain growth polymerisation of TFE leads to PTFE chains in helical arrangements. As a result of this helical structure, the polymer chains exhibit a rod-like behaviour leading to crystallites consisting of large domains of long and highly ordered polymer chains. Therefore, PTFE usually exhibits a high crystallinity degree of up to 95% [29], [32].

With a crystallite melting point of 327 °C, PTFE shows excellent thermal properties and can be exposed to permanent temperatures in the range of -200 to 250 °C without any loss of material properties. For a short time, PTFE is heat-resistant even up to 300 °C, but above 400 °C thermal decomposition occurs with the release of toxic components [32].

Furthermore, PTFE exhibits excellent electrical insulation properties and is therefore highly suitable for use as a wire and cable insulation, as well as PTFE ionomer membranes in fuel cells and electrolysis cells [32].

2.4 Plasma treatment of surfaces

A plasma can be defined as a gas in an excited state comprising atoms, ions, metastable species, free electrons and free radicals that interact with the surface of a substrate [33]. Plasmas can be generated by exposing a gas to an electric field leading to an ionisation process, in which gas atoms are dissociated into free electrons and positively charged ions. Plasmas are electrically conductive, despite maintaining an overall electrical neutrality due to the equal number of positively and negatively charged particles. Furthermore, when an excited species transitions to the ground state, radiation is emitted and a characteristic glow can be observed [34]. Plasmas can be classified as either thermal plasmas or non-thermal ("cold") plasmas based on their process temperature [34], [35]. In thermal plasmas, more than 80% of the plasma energy can be converted into heat and plasma temperatures can reach several thousand Kelvin. While thermal plasmas are used for material processing, such as arc welding, they are usually not suitable for the surface modification of heat sensitive materials [35]. In comparison to thermal plasmas, non-thermal plasmas typically lead to plasma temperatures in the range of 50 to 150 °C also allowing surface treatments of heat sensitive materials. Non-thermal plasmas exhibit significantly lower energy densities than thermal plasmas and the ionisation is primarily maintained by collisions between electrons and neutral particles. Regarding the process pressures, plasmas can be further classified as low-pressure plasmas (0.1 to 5 mbar) or atmospheric plasmas (at atmospheric pressure). Low-pressure plasmas are usually generated by applying a high-frequency alternating current to the electrodes in a vacuum chamber, which can be designed as a cylinder chamber system or a parallel plate reactor. Potential process gases for low-pressure plasmas include oxygen (O₂), hydrogen (H₂), nitrogen (N₂), argon (Ar) and ammonia (NH₃) among others. The following Figure 9 shows the schematic structure of a low-pressure plasma system [36].

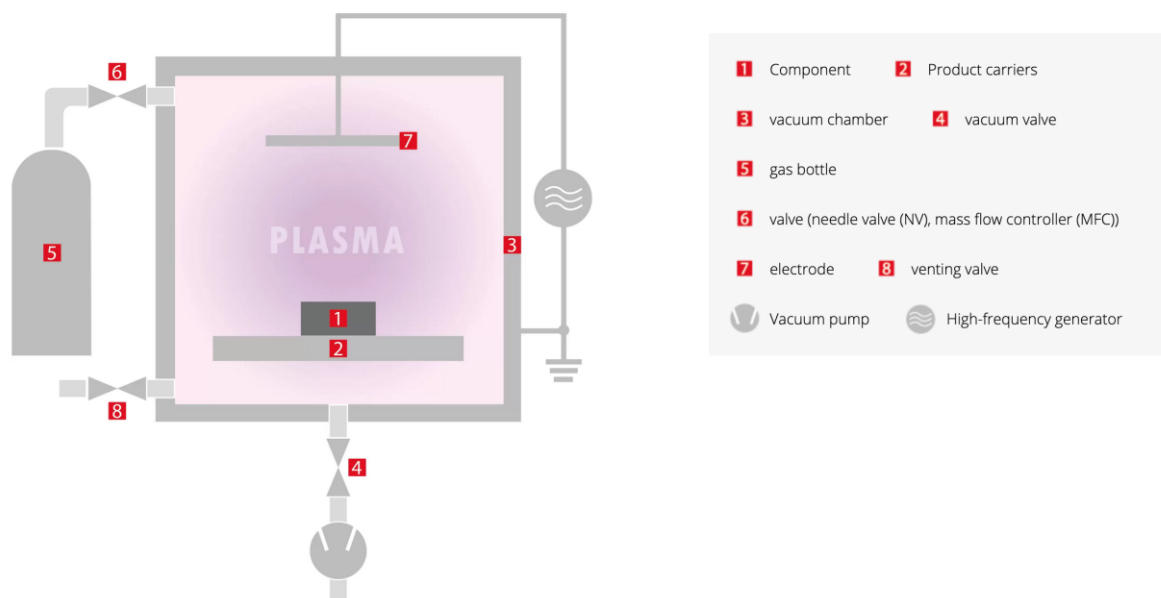


Figure 9: Schematic setup of a low-pressure plasma system [36].

In atmospheric plasmas, the propagation of a plasma within a volume due to impact ionisation is significantly constrained by the short average atomic distances at atmospheric pressure. Therefore, the plasma treatment must be either conducted within close proximity to the substrate or the plasma must be sufficiently powerful to overcome the distance to the substrate surface. Atmospheric plasmas typically comprise air as the process gas [34].

A plasma treatment can lead to different effects, such as:

- Cleaning
- Degradation and ablation
- Crosslinking
- Oxidation
- Polymerisation and grafting onto the substrate surface
- Ion implantation

In case of cleaning, low-molecular contaminations are removed from the substrate surface. If degradation and ablation occur, the plasma removes substrate material from the surface. Additionally, plasma can lead to crosslinking of unsaturated polymers on the surface, although this effect usually only occurs to a minor extent. Oxidation introduces polar groups, such as carbonyl groups, to the surface. Furthermore, a polymerisation of components in the gas phase can occur, which are then deposited on the surface as a thin polymer film and coupled via a “grafting to” reaction. Ions or

foreign atoms can also be implanted into the substrate surface. It is possible, that several of the above-mentioned effects can occur simultaneously [33]. One of the main benefits of employing plasma treatment to substrates is the limitation of the modification to the surface, thus preserving the intrinsic properties of the bulk material. In addition, plasma treatment is a completely dry process in which a variety of different functional groups can be introduced to a surface, depending on the gas used. Furthermore, modification via plasma treatment provides a good homogeneity of the modification across the substrate surface [37]. With regard to plasma treatment, also the so-called hydrophobic recovery has to be considered. Hydrophobic recovery is a thermodynamically driven ageing process the exact mechanism of which is yet to be determined. It is suggested that the polar functional groups, which may be introduced by plasma treatments before, undergo a rotation towards the bulk to minimise the surface free energy [38], [39]. According to Primc et al. [39] hydrophobic recovery progresses rapidly in the first few hours after the plasma treatment and can proceed up to several weeks. However, a certain quantity of functional groups usually persists on the surface, resulting in a final hydrophilicity that is superior compared to an untreated sample, despite the hydrophobic recovery [39].

2.5 Quaternary ammonium compounds

Quaternary ammonium compounds (QACs) are organic amines with the general structure of R_4N^+ . QACs are synthesised from primary, secondary and tertiary amines or ammonia by gradual hydrogen substitution through exhaustive alkylation. (R) stands for the organic residues, which can be alkyl, benzyl, aryl and heteroaryl groups. Due to the presence of four organic residues attached to the nitrogen atom, the nitrogen is positively charged. In comparison to inorganic ammonium (NH_4^+), QACs have a bulkier structure leading to a stronger shielding of the R_4N^+ ion from counterions in a solution. Furthermore, the properties of QACs are also strongly dependent on the nature of the organic residue [40].

QAC characteristics and applications

QACs are solid ionic substances which, unlike amines, contain a permanently positively charged nitrogen atom. Therefore, they exhibit a high solubility in polar and protic solvents such as water or alcohol. However, the solubility of QACs in polar and protic solvents decreases with increasing chain length of (R) while their solubility in nonpolar solvents improves. Furthermore, QACs are ionically conductive making them suitable for the use as electrolytes. Due to their structure containing a polar head (N^+) and nonpolar tails (R) QACs are also used as cationic surfactants. Hereby, they increase the conductivity of a surface and can therefore be used as antistatic agents to prevent spark discharges and dust accumulation. QACs are also suitable for use as herbicides and pesticides due to their desiccating properties. Furthermore, they exhibit antimicrobial activity rendering them suitable for utilisation as antibacterial substances. In principal, QACs can undergo four different reactions, as shown in the following Figure 10: (a) elimination, (b) substitution, (c) rearrangement and (d) ion exchange reactions [40].

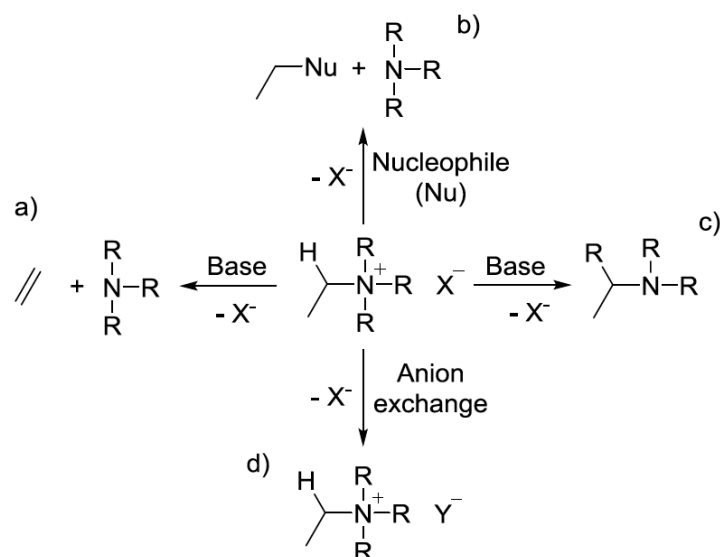
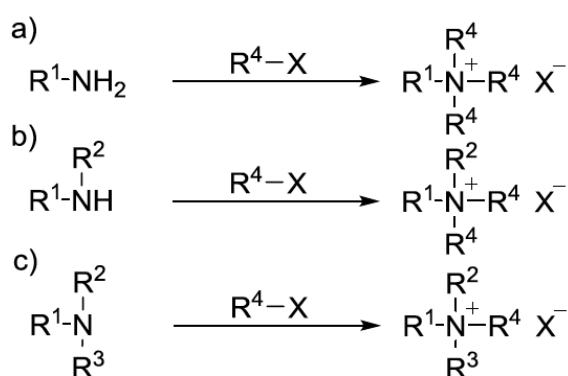


Figure 10: QAC reaction possibilities: (a) elimination, (b) substitution, (c) rearrangement and (d) ion exchange reactions [40].

Due to the wide range of applications and the associated high production figures, the Organisation for Economic Co-operation and Development (OECD) has classified QACs as high-production-volume chemicals. However, in recent years concerns regarding toxicity, accumulation in soil, water and plants, bacterial and antibiotic resistance and health issues such as asthma have been reported [40].

QAC production

QACs can be synthesised from primary, secondary and tertiary amines by exhaustive alkylation as shown in the following Figure 11 [40].



X (R⁴X) = Cl, Br, I, OTs, OH, OSO₃R, O⁺R₂BF₄⁻,

H (alkene)/H⁺, organometal etc.

R = alkyl chain

Figure 11: Quaternisation of (a) primary, (b) secondary and (c) tertiary amines [40].

For the quaternisation of primary and secondary amines sterically hindered organic bases are used as proton acceptors to bind the acid produced during the reaction. In comparison to the amine, the organic base must possess a higher basicity, while also exhibiting a slower reaction rate with the alkylation agent [41]. Tertiary amines are the most convenient starting compound since only one alkyl residue must be coupled to the nitrogen atom to prepare a QAC [40]. The formation of QACs from tertiary amines and haloalkanes is also known as the Menshutkin reaction and follows a S_N2 mechanism [40], [42]. Furthermore, ammonia can also be used as a starting material to produce symmetrical QACs.

In most cases haloalkanes with the general structure of R^4X are used as alkylating agents providing the counterion X^- , which can undergo further ion exchange reactions [40]. A lower bond strength between the alkyl group and the halogen atom of the haloalkane leads to a higher reactivity for the quaternisation. Among the haloalkanes, methyl iodide is particularly suitable for use in quaternisation because it exhibits a low bond energy of 239 kJ/mol and exists in the liquid state at atmospheric pressure and room temperature [42]. Studies by Kleijwegt et al. [42] have found that polar, aprotic solvents increase the quaternisation reaction rates. Hereby, methanol is suggested as the most suitable solvent for quaternisation reactions due to its high reaction rate at higher temperatures, high solubility and low boiling point. In solventless systems it was observed, that the quaternisation reaction rate for tertiary amines decreased with increasing chain length of the alkyl residues. However, for chain lengths exceeding three carbon atoms, the reaction rate remains relatively constant due to a counterbalance of polar and steric effects. For quaternisation reactions conducted with methyl iodide in solution, the steric effects have a predominant influence and the reaction rate decreases with increasing alkyl chain length [42].

2.6 Characterisation methods

X-ray photoelectron spectroscopy (XPS)

X-ray photoelectron spectroscopy (XPS) is one of the most widely used surface analysis techniques. The functionality of XPS is based on the so-called photoelectric effect, in which electrons are emitted from surfaces exposed to electromagnetic radiation. The photoelectric effect was first observed by Heinrich Hertz in 1887 and subsequently formalised by Albert Einstein in 1905. The technology behind today's XPS instruments was developed in the 1950s and 1960s by Kai Siegbahn during his work at the University of Uppsala in Sweden. In XPS, a sample surface is exposed to x-rays and the emitted electron's kinetic energy is measured [43], [44]. The general structure of an XPS measuring device is shown schematically in the following Figure 12 [43].

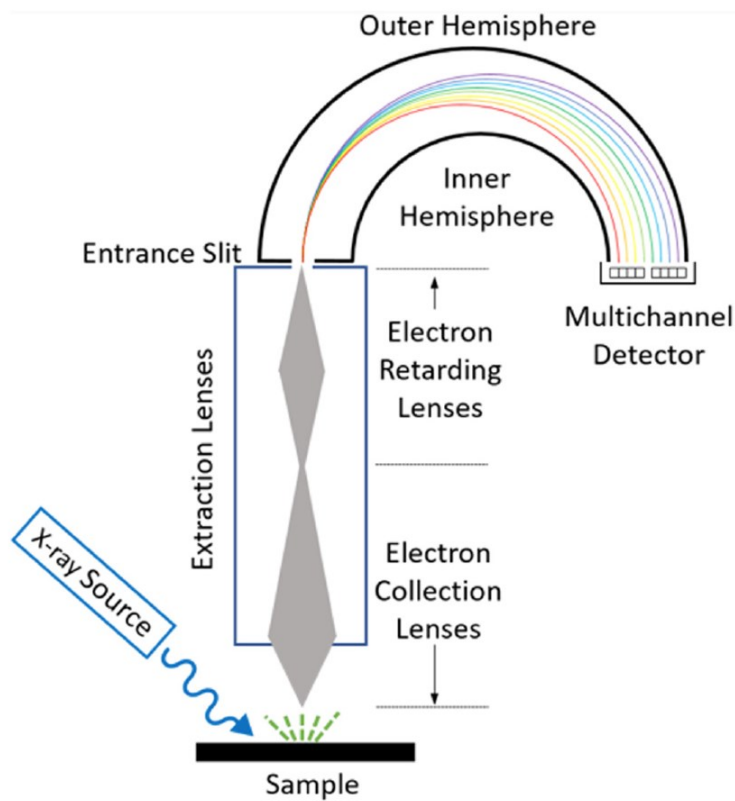


Figure 12: General structure of an XPS measuring device [43].

An XPS measuring device comprises an x-ray source, a sample holder, a set of extraction lenses, an analyser and a detector. All components are enclosed in an ultra-high vacuum (UHV) with pressures typically between 10^{-9} bis 10^{-10} mbar. Hereby, the vacuum prevents surface contamination and the scattering of emitted electrons due to collisions with air molecules. The x-ray source consists of an electron source and a high-voltage anode, towards which the generated electrons are accelerated. The

electron source usually contains a heated tungsten or lanthanum hexaboride (LaB_6) filament. Aluminium or magnesium anodes are typically used as x-ray anodes. Some x-ray sources even contain both types with the option of switching between the respective anodes, whereas XPS devices using a monochromator typically contain an aluminium anode [43]. The use of a monochromator results in the excitation of the sample surface only with x-rays of a specific energy [43], [44]. The energy of the electrons emitted from an x-ray source with a magnesium anode is 1253.6 eV and with an aluminium anode 1486.6 eV, respectively. The extraction lenses, which contain electron-collecting and electron-retarding lenses, are positioned between the sample and the analyser. The electron-collecting lenses are responsible for collecting and focussing the electrons emitted by the sample. The electron-retarding lenses reduce the energy of the emitted electrons to a specific energy level defined by the user, which is also referred to as the pass energy, to achieve a higher spectral resolution. This lower pass energy and therefore higher spectral resolution is primarily required for high-resolution scans, whereas higher pass energies are typically used for survey scans. A survey spectrum provides information about the surface composition while a high-resolution spectrum offers insights about the chemical species present for the respective element. In terms of analysers, so-called concentric hemispherical analysers consisting of an inner and outer hemisphere have become commercially well-established. Different voltages are applied to the two hemispheres, resulting in a greater negative charge on the outer hemisphere. Consequently, high energy electrons collide with the outer hemisphere, while low energy electrons collide with the inner hemisphere. Adjusting the applied voltages enables the passage of electrons with certain energies through the analyser. Furthermore, the higher the radius of the analyser, the higher the resolution [43]. An electron multiplier is typically used as a detector situated at the exit of the analyser to measure the intensity of the emitted electrons [43], [44].

With the exception of hydrogen and helium, XPS can be used to detect all elements on sample surfaces. Hereby, the sample surface is irradiated by x-rays produced by the x-ray source. Electrons close to the core of surface atoms are emitted with a kinetic energy (KE) if the energy of the x-rays ($h\nu$) is higher than the binding energy (BE) of the electrons. If an electron is emitted, the energies are related according to the

following equation (10), where ϕ_{spec} is a constant value known as the spectrometer work function:

$$h\nu = BE + KE + \phi_{spec} \quad (10)$$

Since XPS measures the kinetic energy of an emitted electron and $h\nu$ and ϕ_{spec} are known, equation (10) can be rearranged to determine the binding energy of the electron according to the following equation (11):

$$BE = h\nu - KE - \phi_{spec} \quad (11)$$

Furthermore, the an electron's binding energy is a material property and therefore only the kinetic energy will vary depending on the energy of the x-ray source. The emission of an electron close to the core of a surface atom creates a "core hole" in its energy band, which is filled by an electron from a valence orbital in a relaxation process. This electron transfer again leads to an energy release, which results in either x-ray fluorescence or the emission of a so-called Auger electron. Since x-ray fluorescence is not considered in XPS measurements, it will not further be discussed within the scope of this work. The processes of x-ray induced emission of an XPS electron and an Auger electron are shown in the following Figure 13 [43].

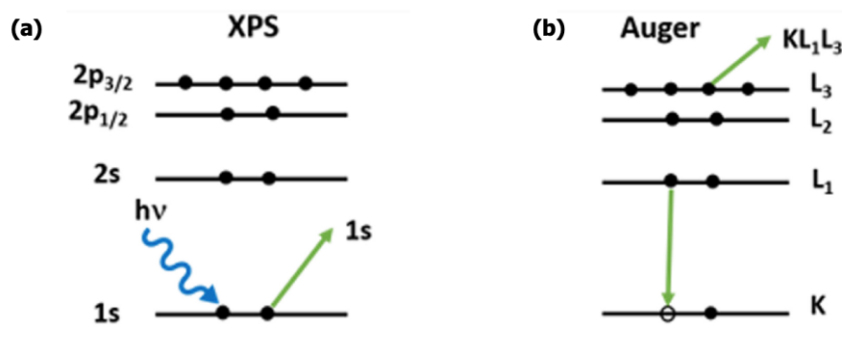


Figure 13: X-ray induced emission of an (a) XPS electron and (b) Auger electron [43].

As shown in Figure 13 above, the XPS electron peak is designated according to element and orbital from which the electron is emitted. The Auger electron peak is named according to the K, L and M atomic orbital classification. The first letter designates the orbital from which the XPS electron was emitted, the second letter describes the origin

of the electron that filled the core hole and the third letter stands for the orbital from which the Auger electron is released. X-rays are usually able to penetrate the sample surface up to depth of a few micrometers (μm) also leading to an electron emission below the surface. The released electrons then proceed to move through the bulk material to the surface and might gradually lose their kinetic energy due to inelastic collisions. Electrons experiencing many inelastic collisions might lose all their kinetic energy and are therefore not detectable by XPS. Furthermore, electrons emerging from the sample surface with reduced kinetic energy due to only a few inelastic collisions are usually detectable and determine the vertical level of the background signal. The characteristic peaks used in XPS analysis are produced by electrons that do not experience any inelastic collisions on their way towards the detector. Therefore, the common sampling depth or information depth for XPS measurements is considered to be ≤ 10 nm [43].

XPS data is typically plotted in a so-called XPS spectrum. In such spectrum, the binding energy in electronvolt (eV) is displayed along the horizontal axis in decreasing order and the intensity in counts per second (cps) along the vertical axis as shown in the illustrative spectrum in the following Figure 14 [43].

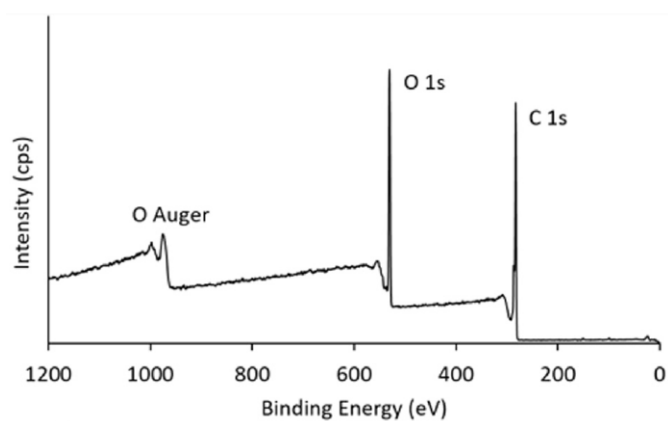


Figure 14: Exemplary XPS-spectrum [43].

Each element possesses a characteristic binding energy, enabling XPS to be used in combination with databases and literature to identify and quantify surface compositions. Furthermore, the chemical bonding state can also be analysed under the condition that the elements involved exhibit different electronegativities. A chemical bond leads to a shift in the involved electron binding energies which results in a peak shift also known as a chemical shift [44].

3 Experimental

3.1 Chemicals, materials and equipment

The following Table 1 contains all chemicals used in the experiments of this work.

Table 1: List of used chemicals.

Chemical	CAS Registry Number	Purity	Manufacturer
Ethanol absolute	64-17-5	≥99.5%	VWR International S.A.S., Radnor, Pennsylvania, USA
Ethyl acetate	141-78-6	≥99.5%	Carl Roth GmbH + Co. KG, Karlsruhe, Germany
Methanol	67-56-1	≥99.9%	Carl Roth GmbH + Co. KG, Karlsruhe, Germany
(3-Aminopropyl) Triethoxysilane "APTES"	919-30-2	≥98%	Sigma-Aldrich Co., St. Louis, Missouri, USA
2-Dimethylaminoethyl acrylate "DMAEA"	2439-35-2	98%	Sigma-Aldrich Co., St. Louis, Missouri, USA
N,N-Dimethyl-4- vinylaniline "DMVA"	2039-80-7	97%	Abcr GmbH, Karlsruhe, Germany
Tributylamine	102-82-9	≥98%	Tokyo Chemical Industry Co., Ltd., Tokyo, Japan

Methyl iodide	74-88-4	99.5%	Sigma-Aldrich Co., St. Louis, Missouri, USA
Silica nanopowder	7631-86-9	99.8%	Sigma-Aldrich Co., St. Louis, Missouri, USA

For the sake of clarity, the following abbreviations are used for the chemical substances in Table 1:

APTES ... (3-Aminopropyl)triethoxysilane

DMAEA ... 2-Dimethylaminoethyl acrylate

DMVA ... N,N-Dimethyl-4-vinylaniline

Furthermore, all materials used in the experiments of this work are listed in the following Table 2. PTFE films with a thickness of 0.1 mm and the dimensions of 1.5 x 1.5 cm or PTFE particles with a diameter of 6-9 μm were used as substrates for the surface treatment.

Table 2: List of materials used in the experiments.

Material	Product Code	Manufacturer
PTFE particles 6-9 μm	FP30-PD-000110	Goodfellow Cambridge Limited, Huntingdon, England
PTFE film 0.1 mm	FP30-FM-000300	Goodfellow Cambridge Limited, Huntingdon, England

The following Table 3 contains a list of all devices used in the experiments of this work.

Table 3: List of used devices.

Device	Model name	Manufacturer
Plasma device	Tetra 30	Diener electronic GmbH + Co. KG, Ebhausen, Germany
Plasma device	Tetra 100	Diener electronic GmbH + Co. KG, Ebhausen, Germany
Plasma device	Femto-BR-200-PCCE7-c	Diener electronic GmbH + Co. KG, Ebhausen, Germany
Screw cap bottle Duran®	100 ml / 2000 ml	DWK Life Sciences, Wertheim, Germany
Kapton® tape	10 - 15 mm	cmc Klebtechnik GmbH, Frankenthal, Germany
Magnetic stirrer with heating	C-MAG HS 7	IKA®-Werke GmbH & Co. KG, Staufen, Germany
Temperature controller	ETS-D5	IKA®-Werke GmbH & Co. KG, Staufen, Germany
Analytical scale	MSA225P	Sartorius AG, Göttingen, Germany
Piston-stroke pipette	Tacta 1000	Sartorius AG, Göttingen, Germany
Piston-stroke pipette	Tacta 200	Sartorius AG, Göttingen, Germany

Centrifuge	Heraeus™ Labofuge 300	Thermo Fisher Scientific Inc., Waltham, Massachusetts, USA
Ultrasonic bath	Sonorex Digitec	BANDELIN electronic GmbH & Co. KG, Berlin, Germany
Drying chamber	ED 53	BINDER GmbH, Tuttlingen, Germany
XPS	Nexsa G2	Thermo Fisher Scientific Inc., Waltham, Massachusetts, USA

3.2 Sample preparation

The following Figure 15 shows the strategic flow chart for the PTFE functionalisation techniques used within the scope of this thesis. Fundamentally, the functionalisation of the PTFE particles was conducted as a three-step process consisting of the activation of the particle surface, the introduction of amino groups to the surface and quaternisation of these amino groups.

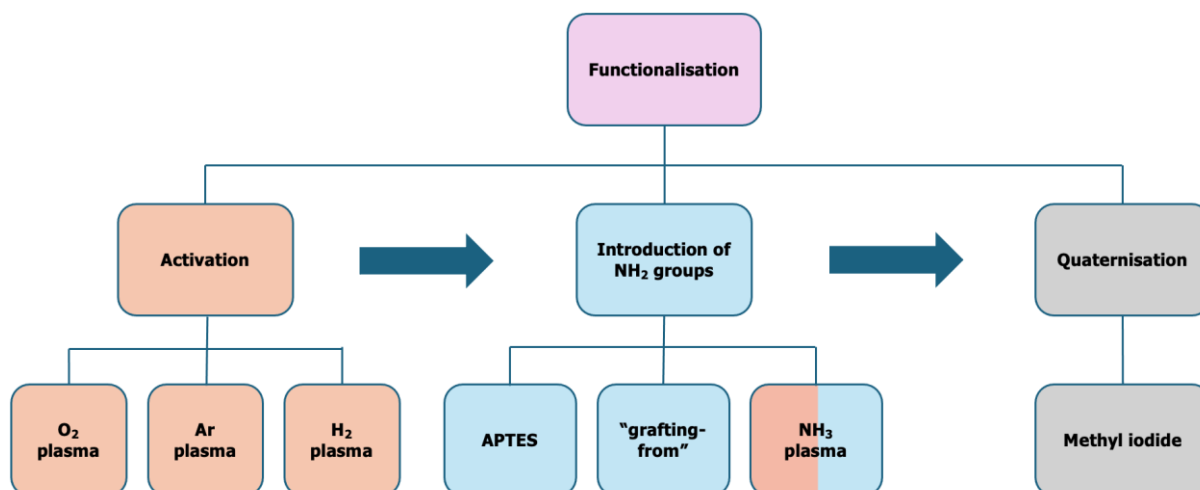


Figure 15: Strategic flow chart for the PTFE particle functionalisation.

Activation via O₂, Ar or H₂ plasma and introduction of amino groups via APTES

First, 1 g of the PTFE particles was weighed in using the analytical scale. The particles were then transferred into a screw cap bottle, which was modified with folded strips of Kapton[®] tape inside the bottle to support a sufficient mixing and uniform particle surface treatment, as seen in the following Figure 16.



Figure 16: Folded Kapton[®] tape strips inside a screw cap bottle.

The bottle was mounted around a rod electrode using the rotating bottle holder inside the Tetra 30 plasma chamber. Hereby, either an 8 cm long electrode in combination with a 100 ml bottle or a 22 cm long electrode in combination with a 2000 ml bottle were used. Despite the different lengths, both electrodes exhibited the same diameter of 1.8 cm. After the door was closed, the chamber was evacuated to a pressure of approximately 0.03 mbar. As soon as the vacuum pressure was constant, a controlled flow of oxygen, argon or hydrogen gas was fed to the chamber and the internal chamber pressure was set to 0.3 mbar. Although the Tetra 30 plasma system has a rated power of 1000 W, the maximum power when using the 8 cm long electrode is limited to 30% of the rated power due to geometrical constraints. Therefore, the plasma power was set to either 300 W or 1000 W depending on the electrode configuration and a corresponding high voltage was applied to the electrodes creating the plasma. The duration of the treatment was varied according to the following Table 4.

Table 4: O₂, Ar or H₂ plasma treatment durations.

Plasma	Duration [min]			
	10	20	30	60
O ₂	10	20	30	60
Ar	10	60	-	-
H ₂	10	-	-	-

After the PTFE particles were plasma treated for defined time periods, the particles were transferred from the bottle into a vial and dispersed in an APTES solution. Hereby, a 10.2 ml APTES solution containing ethanol absolute and distilled water in a ratio of 9:1 and 2 vol% APTES was prepared using the piston-stroke pipettes. The vial was placed on the magnetic stirrer at room temperature or with the heater and temperature controller set to 50 °C for 24 hours. After the treatment with APTES, the dispersed particles were transferred into a centrifuge tube and centrifuged at 4000 rpm for 30 minutes to separate the particles from the reaction solution. Then the APTES solution was drained followed by the rinsing and dispersion of the particles in ethanol absolute with a spatula inside the centrifuge tube. The tube was then immersed in the ultrasonic bath for 5 minutes before the particles were again centrifuged at 4000 rpm for 30 minutes. This cleaning process was repeated three times and after each centrifugation cycle the ethanol absolute was renewed. After the last cleaning cycle, the ethanol absolute was removed and the particles were transferred from the centrifuge tube into a vial and dried for 24 hours using a drying chamber set to 150 °C. After the drying time was completed, the vial containing the particles was removed from the oven and sealed with a screw cap.

Activation via Ar plasma and introduction of amino groups via “grafting-from” reaction

Similar to the process described before, approximately 1 g of PTFE particles was filled into the 2000 ml screw cap bottle modified with Kapton® tape and mounted around the 22 cm long rod electrode inside the Tetra 30 plasma device. After the evacuation step and pressure drop to 0.03 mbar, a controlled flow of argon gas was fed into the chamber and the internal chamber pressure was set to 0.3 mbar. Hereby, the plasma power was set to 1000 W for a duration of either 10 or 20 minutes. Afterwards, a pure monomer or monomer solution was filled into a vial using the piston-stroke pipettes followed by the dispersion of the particles. The monomers used were DMAEA (10 ml pure monomer or 10.2 ml solution of ethylacetate with 2 vol% DMAEA) or DMVA (10.2 ml solution of 9:1 ethanol absolute and distilled water with 2 vol% DMVA). The vial containing the particles and monomer or monomer solution was then placed on the magnetic stirrer at room temperature for 35 minutes. In the next step, the dispersed particles were transferred into a centrifuge tube and centrifuged at 4000 rpm

for 30 minutes. Subsequently, the reaction solution was removed, the particles were rinsed and dispersed in the respective solvents (ethylacetate for DMAEA or ethanol absolute for DMVA) with a spatula within the centrifuge tube. Furthermore, the tube was immersed in the ultrasonic bath for 5 minutes before the particles were again centrifuged at 4000 rpm for 30 minutes. This cleaning process was repeated three times and the solvent was renewed between each cleaning step. Afterwards, the particles were transferred into a vial and dried for 24 hours using a drying chamber set to 150 °C. After the drying time was completed, the vial containing the particles was removed from the oven and sealed with a screw cap.

Activation and introduction of amino groups via NH₃ plasma

For this process, 3 g of PTFE particles were spread on a plate electrode inside a Tetra 100 plasma device at the Diener electronic GmbH + Co. KG company site. The pressure was set to 0.25 mbar and a controlled flow of NH₃ gas was fed into the chamber. Hereby, the plasma treatment was conducted at two different power settings for different time periods according to the following Table 5.

Table 5: NH₃ plasma power and treatment durations.

Plasma power [W]	Duration [h]	
1000	1	3
3000	1	-

Half of the plasma treated particles was stored in vials containing air while the other half was stored in vials containing ethanol absolute.

Quaternisation

First, 0.5 g of the NH₃ plasma treated particles were weighed using the analytical scale. Furthermore, a solution containing 5 ml methanol, 0.3 ml tributylamine and 0.5 ml methyl iodide was prepared in a vial using the piston-stroke pipettes followed by the dispersion of the particles in the solution with a spatula. The dispersion was either left to rest or stirred for six hours using the magnetic stirrer at room temperature. For the non-stirred particles, a large fraction of the solution was removed from the vial with a disposable pipette and the particles were transferred into a centrifuge tube filled with

ethanol absolute. The stirred particles were also transferred into a centrifuge tube and centrifuged at 4000 rpm for 30 minutes. After the reaction solution was decanted, ethanol absolute was added to the centrifuge tube. Then, the particles were dispersed in the ethanol absolute with a spatula, the centrifuge tube was closed and immersed in the ultrasonic bath for 5 minutes. The particles were centrifuged at 4000 rpm for 30 minutes for three cycles and the ethanol absolute was renewed between each cycle. Afterwards, the particles were transferred from the centrifuge tube into a vial and were dried at 100 °C for 24 hours in the drying chamber. After the drying time was completed, the vial containing the particles was removed from the oven and sealed with a screw cap.

3.3 Characterisation

X-ray photoelectron spectroscope (XPS)

The surface composition of the PTFE particles was determined via a Nexsa G2 X-ray photoelectron spectroscope (XPS) by Thermo Fisher Scientific Inc. using Al K- α radiation (at 1486.8 eV) at room temperature. Hereby, the particles were fixed to an XPS sample holder using double-sided adhesive carbon tape. Once the sample holder was successfully positioned within the measuring chamber, a survey scan at a pass energy of 200 eV and an energy resolution of 1.0 eV was conducted. Furthermore, hydrogen was not taken into account for the calculation of the surface composition. Per sample a minimum of two measuring points were examined and the results were evaluated using the associated software "Advantage".

4 Results and discussion

The use of plasmas is well suited for surface activation and functionalisation since this treatment is known for its ability to introduce functional groups to surfaces, which in turn affect the polarity of the treated surfaces or serve as binding sites in further modification reactions [33], [37]. As a pre-treatment method, gaseous plasmas have gained popularity, especially for fluorine-free polymers, but also the application to fluoropolymers is being researched [1]. In this work, PTFE particles were functionalised by plasma-based techniques in order to introduce the required ion conductivity for the use as a binder in AEM water electrolysis cells. Therefore, O_2 , Ar and H_2 plasmas were applied to introduce binding sites for the subsequent coupling of amino silanes. Alternatively, a NH_3 plasma was applied aiming the direct introduction of amino groups to the surface. Finally, these amino groups were quaternised to introduce anion conductivity to the PTFE substrates. After an XPS reference measurement was conducted to determine the surface composition of the untreated PTFE particles, each modification step was followed by XPS measurements, investigating the changes in surface composition.

Surface modification via plasma treatment and subsequent silanisation with APTES

In a first approach, O_2 plasma and a subsequent coupling of (3-Aminopropyl)triethoxysilane (APTES) was used to attach amino moieties to the PTFE substrates. O_2 plasma results in the formation of polar oxygen-containing species on the surface, including -OH, -COOH and -C=O groups, and radicals, which likely include alkoxy radicals ($O\cdot$) as well as peroxy radicals ($ROO\cdot$) [37]. The resulting functional groups increase the surface free energy and act as coupling sites for further treatments. The following Figure 17 illustrates the functionalisation of a PTFE substrate via O_2 plasma.

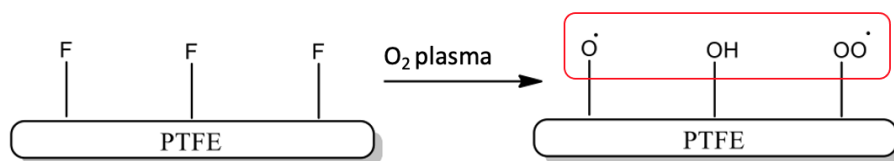


Figure 17: PTFE functionalisation via O_2 plasma.

The subsequent coupling of APTES follows a reaction mechanism shown in Figure 18, where APTES first undergoes a hydrolysis reaction in the solution before being coupled to the PTFE surface by absorption and condensation reactions.

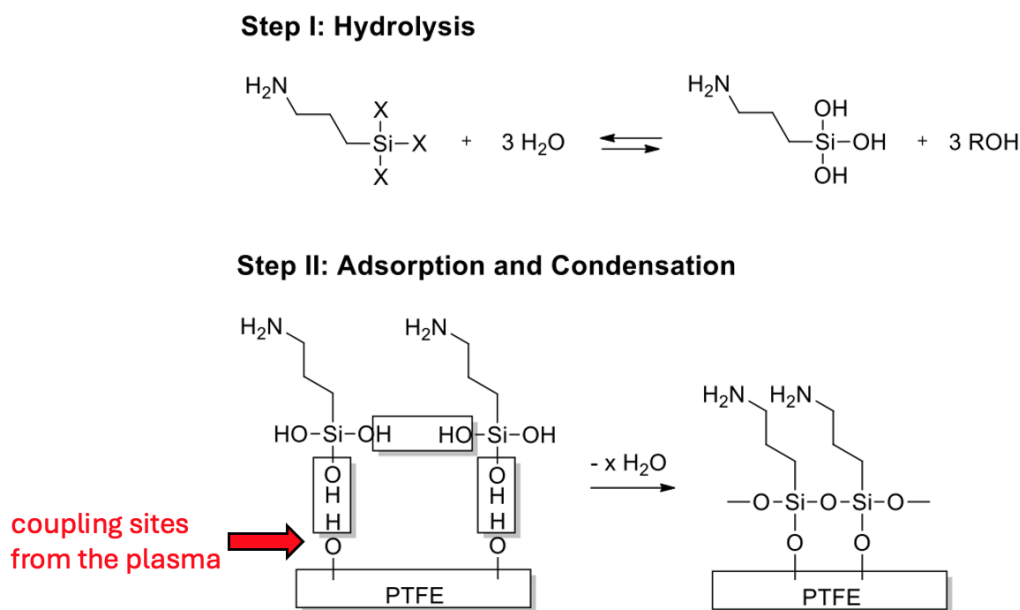


Figure 18: Two-step coupling of APTES to PTFE surfaces.

In the initial phase of the study, the PTFE particles were treated with O_2 plasma at a power of 300 watts and varying the treatment duration (see Table 6), after which they were immediately analysed by XPS. The results in Table 6 show, that no oxygen-containing functional groups could be detected on the surface independent of the plasma duration. This can be due to the phenomenon of hydrophobic recovery (see section 2.4), in which polar functional groups on a substrate's surface rotate into the bulk material [38]. However, experience with PTFE films in the bachelor thesis of Sebastian Ernst, BSc has shown that APTES can still be coupled to PTFE surfaces by this method. Therefore, functional groups can exist on the substrate, even if not detectable via XPS directly after plasma treatments. Subsequently, PTFE particles were treated with O_2 plasma followed by APTES varying the plasma power (300 or 1000 watts), the plasma treatment duration and the APTES treatment temperature (room temperature "RT" or $50\text{ }^\circ\text{C}$) according to Table 6. As the results in Table 6 show, the PTFE particle surfaces do not contain nitrogen after the 24-hour APTES treatment but rather resemble the reference composition. Therefore, it was concluded, that the coupling of APTES after O_2 plasma treatment was not successful, independent of the

plasma power and plasma treatment duration and the previously developed modification process could not be easily transferred from PTFE films to particles.

Table 6: XPS results of PTFE particles directly after O₂ plasma and after O₂ plasma and subsequent modification with APTES.

Parameters	F [at.%]	O [at.%]	C [at.%]	N [at.%]	Si [at.%]
Untreated particles	68.3 ± 0.9	-	31.7 ± 0.9	-	-
O₂, 300 W, 10 min	67.6 ± 1.1	-	32.4 ± 1.1	-	-
O₂, 300 W, 20 min	66.9 ± 1.1	-	33.1 ± 1.1	-	-
O₂, 300 W, 30 min	66.8 ± 0.3	-	33.2 ± 0.3	-	-
O₂, 300 W, 10 min, APTES RT	66.5 ± 0.6	-	33.5 ± 0.6	-	-
O₂, 300 W, 20 min, APTES RT	66.9 ± 0.6	-	33.1 ± 0.6	-	-
O₂, 300 W, 30 min, APTES RT	66.7 ± 0.8	-	32.8 ± 0.1	-	-
O₂, 300 W, 60 min, APTES RT	68.5 ± 0.5	-	31.5 ± 0.5	-	-
O₂, 1000 W, 10 min, APTES 50 °C	68.2 ± 0.4	-	31.8 ± 0.4	-	-
O₂, 1000 W, 60 min, APTES 50 °C	68.1 ± 0.2	-	31.9 ± 0.2	-	-

It is notable that in all tables presented in section 4, all element contents measured by XPS are the averaged values derived from two or three measuring points (P1 – P3) per sample. Hereby, “*” labels single values obtained from only one measuring point. Furthermore, treatment with non-oxygen-containing plasma (e.g. Ar and H₂) will also result in the incorporation of oxygen and the formation of oxygen-containing functional groups on the PTFE surface. This is achieved by the formation of free radicals on the surface due to the plasma treatment, which subsequently react with oxygen and moisture present in the ambient air upon opening the plasma chamber [45]. As concluded by Wilson et al. [46] a larger quantity of fluorine is removed from the PTFE surface by treatment with Ar plasma instead of O₂ plasma. Subsequently, the defluorinated radical sites react with oxygen and moisture from the ambient air by chemisorption again forming oxygen-containing functional groups on the PTFE surface, as shown in the following Figure 19 [46].

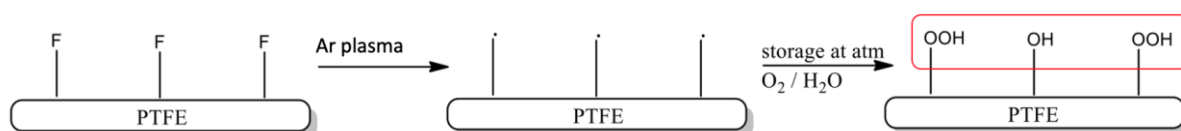


Figure 19: PTFE functionalisation via Ar plasma.

Therefore, the O₂ plasma was replaced by Ar plasma and the plasma power and treatment duration were varied, as shown in the following Table 7. After the plasma treatment, the particles were dispersed in APTES at 50 °C for 24 hours. Hereby, XPS measurements were conducted directly after the plasma as well as after the APTES treatment. As the results in Table 7 show, no oxygen containing functional groups were detected directly after Ar plasma, which may be attributed to hydrophobic recovery (see section 2.4). Furthermore, no nitrogen was detectable after the APTES treatment, independent of the plasma power and treatment duration. The oxygen content of 0.7 ± 0.6 at.% detected on the particle surface after a 10-minute Ar plasma treatment followed by dispersion in APTES leads to the assumption of the presence of oxygen containing functional surface groups other than -OH moieties, which would enable APTES binding. However, since the amount of introduced oxygen species was very small at all, a detailed analysis of the XPS data to identify the exact species was not conducted.

Table 7: XPS results of PTFE particles directly after Ar plasma and after Ar plasma and subsequent modification with APTES.

Parameters	F [at.%]	O [at.%]	C [at.%]	N [at.%]	Si [at.%]
Untreated particles	68.3 ± 0.9	-	31.7 ± 0.9	-	-
Ar, 300 W, 10 min	68.9 ± 0.0	-	31.1 ± 0.0	-	-
Ar, 1000 W, 10 min	68.7 ± 0.6	-	31.3 ± 0.6	-	-
Ar, 300 W, 10 min, APTES 50 °C	67.6 ± 0.2	0.7 ± 0.6	31.8 ± 0.4	-	-
Ar, 1000 W, 10 min, APTES 50 °C	68.8 ± 0.1	-	31.3 ± 0.1	-	-
Ar, 1000 W, 60 min, APTES 50 °C	68.1 ± 0.3	-	31.9 ± 0.3	-	-

The following Figure 20 shows the XPS survey spectra of the PTFE particles treated with O₂ or Ar plasma, each treated at 1000 watts for 10 minutes and dispersed in APTES at 50 °C for 24 hours, as well as the reference measurement of the untreated particles.

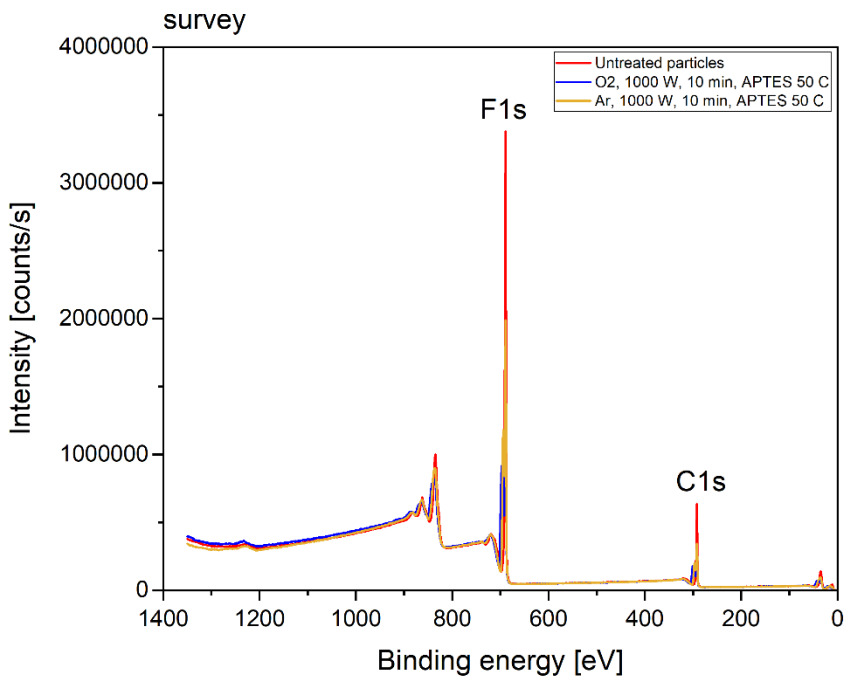


Figure 20: XPS spectra of the PTFE film after O₂ or Ar plasma (1000 W, 10 min) and subsequent modification with APTES and the reference measurement.

As the XPS survey spectrum in Figure 20 shows, the particle surface after the O₂ or Ar plasma and subsequent APTES treatment resembles the untreated reference surface composition.

In order to demonstrate that the activation of PTFE surfaces by O₂ or Ar plasma and subsequent introduction of NH₂ groups by APTES works in general with our equipment, PTFE films with a thickness of 0.1 mm were treated with O₂ or Ar plasma for 10 minutes varying the plasma power followed by the APTES treatment at 70 °C for 24 hours (see Table 8). XPS measurements were conducted after the APTES treatment (BC = before cleaning) as well as after an additional cleaning in ethanol absolute for 5 minutes using the ultrasonic bath (AC = after cleaning).

Table 8: XPS results of PTFE films after O₂ or Ar plasma and APTES before/after cleaning in ethanol absolute.

Parameters	F [at.%]	O [at.%]	C [at.%]	N [at.%]	Si [at.%]
Untreated film	66.4 ± 0.2	-	33.6 ± 0.2	-	-
O₂, 300 W, 10 min, APTES 70 °C, BC	2.9 ± 3.9	25.2 ± 0.7	46.5 ± 1.4	1.7 ± 0.1	23.7 ± 1.7
O₂, 300 W, 10 min, APTES 70 °C, AC	3.9 ± 0.5	20.7 ± 0.3	60.4 ± 1.1	4.6 ± 0.0	8.4 ± 0.3
O₂, 1000 W, 10 min, APTES 70 °C, BC	15.2 ± 4.6	17.4 ± 1.7	54.9 ± 2.5	3.7 ± 0.5	8.8 ± 1.3
O₂, 1000 W, 10 min, APTES 70 °C, AC	3.0 ± 1.8	32.6 ± 2.9	40.6 ± 1.2	7.0 ± 0.8	16.9 ± 0.7
Ar, 300 W, 10 min, APTES 70 °C, BC	-	35.5 ± 2.3	39.2 ± 1.9	5.7 ± 0.5	19.6 ± 0.9
Ar, 300 W, 10 min, APTES 70 °C, AC	1.0 ± 0.2	37.8 ± 2.0	35.9 ± 2.0	6.0 ± 0.1	19.5 ± 0.2
Ar, 1000 W, 10 min, APTES 70 °C, BC	-	35.9 ± 0.3	38.4 ± 0.6	6.8 ± 0.4	18.6 ± 0.2
Ar, 1000 W, 10 min, APTES 70 °C, AC	-	35.7 ± 0.4	38.6 ± 0.0	6.8 ± 0.1	18.9 ± 0.4

As the nitrogen contents in Table 8 show, functional groups were successfully coupled to the surface of the PTFE films. In both cases (O₂ and Ar plasma) the fluorine content was significantly reduced, whereas for Ar treated samples no fluorine was detected anymore before cleaning. This can either indicate a strong defluorination of the substrate by the plasma treatment or the development of an APTES layer exceeding the penetration depth of XPS (≤ 10 nm) [43]. The PTFE film samples treated with O₂

or Ar plasma at 300 watts support the hypothesis of APTES layer formation, as there was an increase in the fluorine content after cleaning. This can be attributed to the removal of uncoupled APTES monomers during the cleaning and therefore fluorine detection from the underlying substrate. Thus, the results show that Ar plasma is even more effective than O₂ plasma to form oxygen containing functional species at the substrate surface which serve as coupling sites for APTES. The following Figure 21 and Figure 22 show the XPS spectra of PTFE films treated with O₂ or Ar plasma at 1000 watts for 10 minutes, respectively, followed by the APTES treatment at 70 °C for 24 hours.

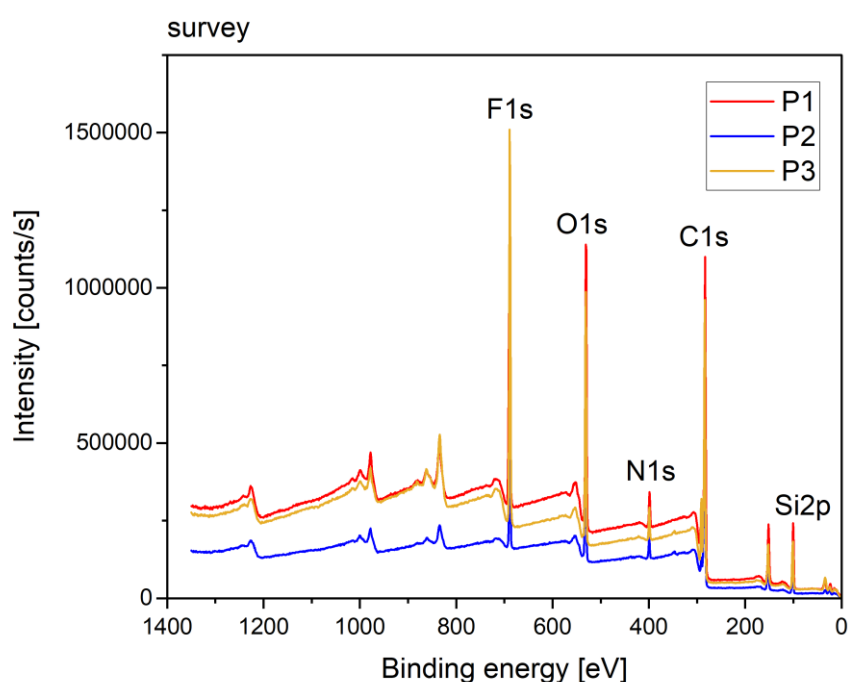


Figure 21: XPS spectra of the PTFE film after O₂ plasma (1000 W, 10 min) and subsequent modification with APTES.

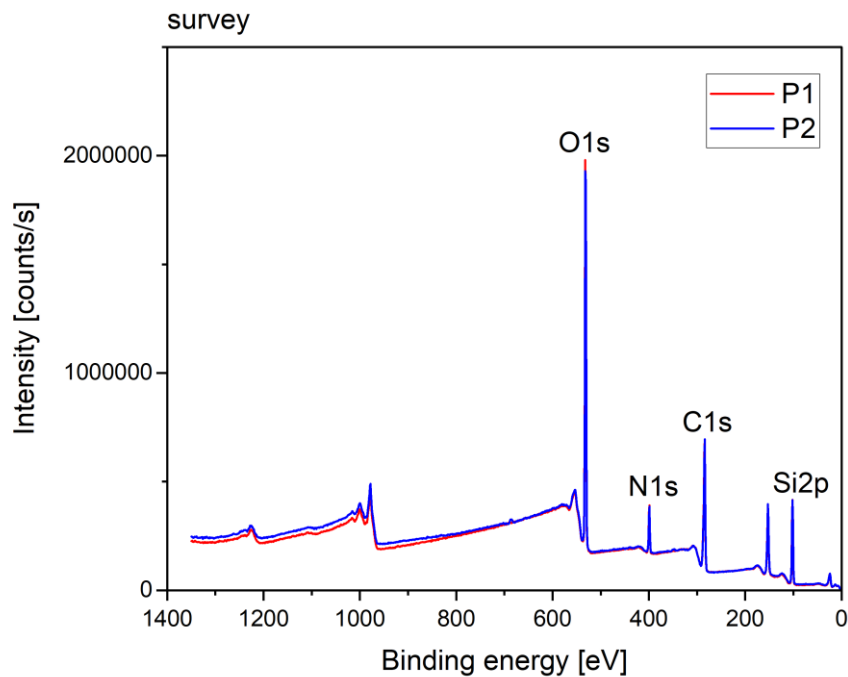


Figure 22: XPS spectra of the PTFE film after Ar plasma (1000 W, 10 min) and subsequent modification with APTES.

In addition, silica (SiO_2) nanopowder was treated with O_2 plasma to verify the process applicability to particles. According to the results in the following Table 9, the plasma treatment at 1000 watts for 10 minutes and dispersion in APTES at 50 °C for 24 hours led to a nitrogen content of 2.8 ± 0.0 at.% and therefore successful APTES coupling.

Table 9: XPS results of SiO_2 particles after O_2 plasma (1000 W, 10 min) and subsequent modification with APTES.

Parameters	F [at.%]	O [at.%]	C [at.%]	N [at.%]	Si [at.%]
O_2, 1000 W, 10 min, APTES 50 °C	-	51.8 ± 0.8	16.0 ± 1.1	2.8 ± 0.0	29.4 ± 0.4

Furthermore, the following Figure 23 demonstrates the XPS spectra of the SiO₂ particles treated with O₂ plasma and APTES.

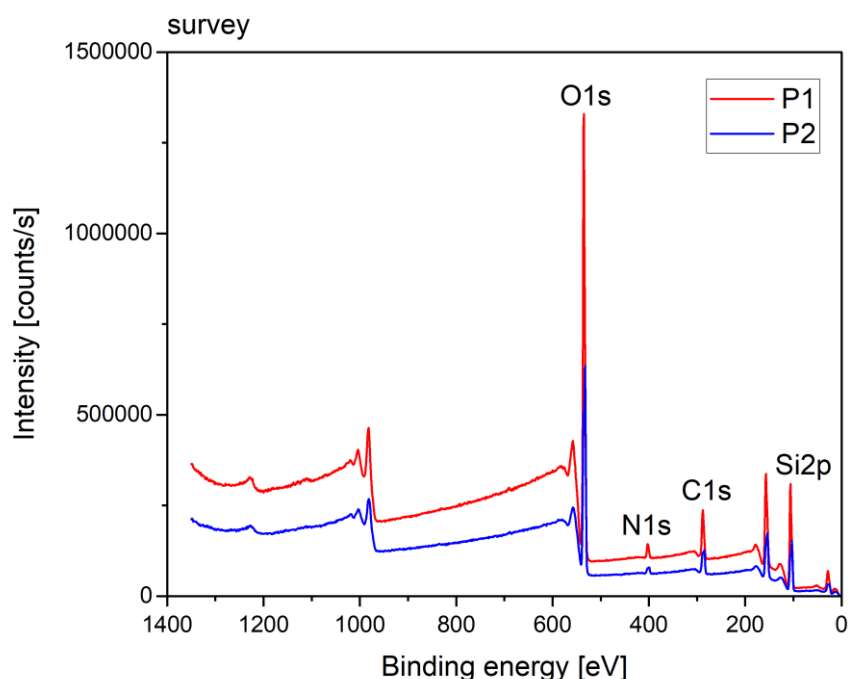


Figure 23: XPS spectra of SiO₂ particles after O₂ plasma (1000 W, 10 min) and modification with APTES.

Another approach is based on the work of Badey et al. [47], who showed that also the treatment with H₂ plasma leads to defluorination at high degrees similar to NH₃ plasma. As shown in the following Figure 24, treatment with H₂ plasma leads to free radical formation, which then react either with hydrogen radicals from the plasma forming C-H bonds or with oxygen and moisture from the ambient air to form hydroxyl and carbonyl groups after opening the plasma chamber [45].

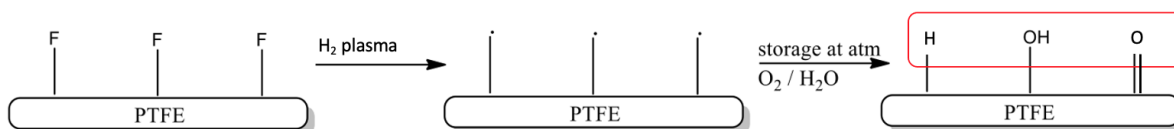


Figure 24: PTFE functionalisation via H₂ plasma.

Therefore, PTFE particles were treated with H₂ plasma at 1000 watts for 10 minutes followed by the dispersion in APTES at 50 °C for 24 hours (see Table 10).

Table 10: XPS results of PTFE particles after H₂ plasma (1000 W, 10 min) and subsequent modification with APTES.

Parameters	F [at.%]	O [at.%]	C [at.%]	N [at.%]	Si [at.%]
Untreated particles	68.3 ± 0.9	-	31.7 ± 0.9	-	-
H ₂ , 1000 W, 10 min, APTES 50 °C	60.6 ± 4.2	3.0 ± 1.9	34.1 ± 0.9	1.2 ± 0.7	1.6 ± 0.1

According to the results in Table 10, the oxygen, nitrogen and silicon contents show that APTES was successfully coupled to the PTFE particle surface. The following Figure 25 shows the XPS spectra of the PTFE particles treated with H₂ plasma at 1000 watts for 10 minutes and APTES at 50 °C for 24 hours versus the reference measurement of the untreated particles.

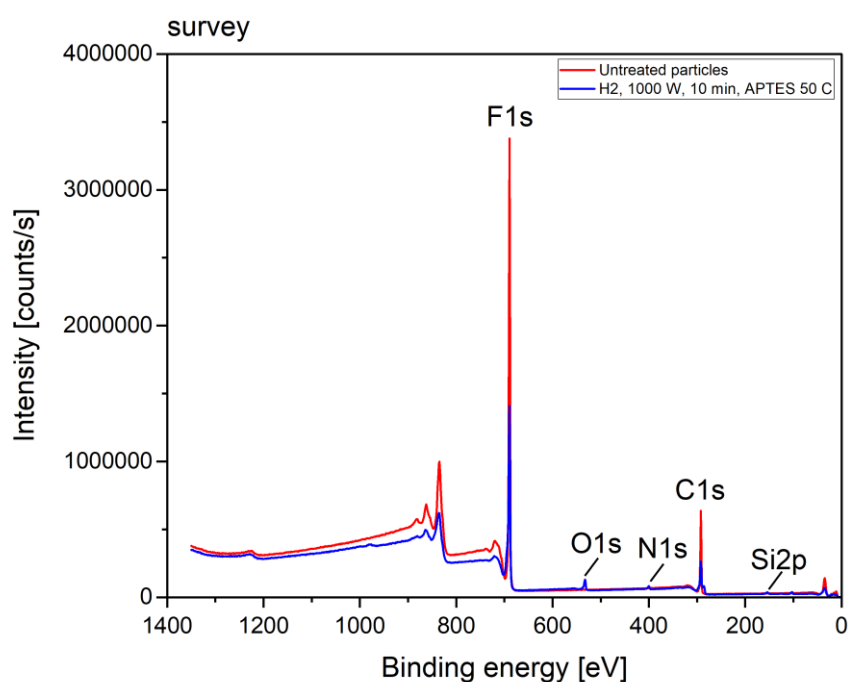


Figure 25: XPS spectra of the PTFE film after H₂ plasma (1000 W, 10 min) and subsequent modification with APTES vs. the reference measurement.

Surface modification via Ar plasma and subsequent “grafting-from” reactions

An alternative approach was a surface activation via Ar plasma and subsequent “grafting-from” reaction of either 2-Dimethylaminoethyl acrylate (DMAEA) or N,N-Dimethyl-4-vinylaniline (DMVA) to introduce amino groups to the PTFE surfaces. For this purpose, the monomers were brought into contact with the activated substrates directly after plasma treatment. The following Figure 26 shows the structural formulas of DMAEA and DMVA [48], [49].

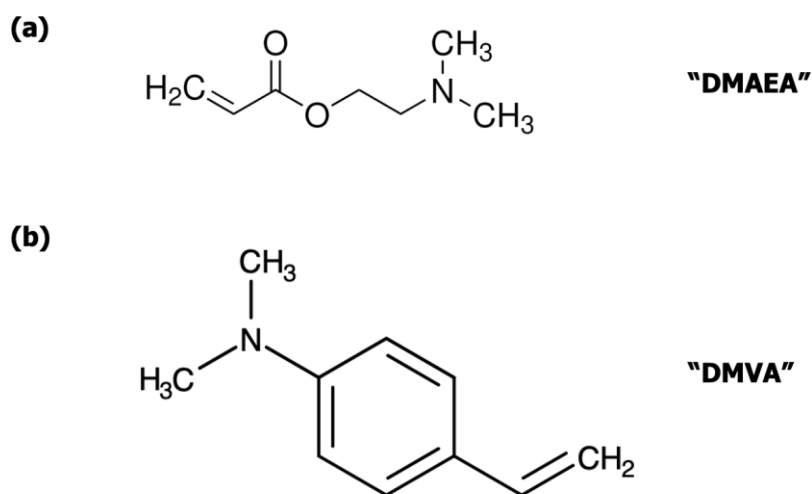


Figure 26: Structural formula of (a) DMAEA [48] and (b) DMVA [49].

As shown in Figure 27, the reactive sites on the PTFE surface were suggested to react with the respective monomer according to a free radical polymerisation, although the “grafting-from” reaction competes with reactions with the ambient air.

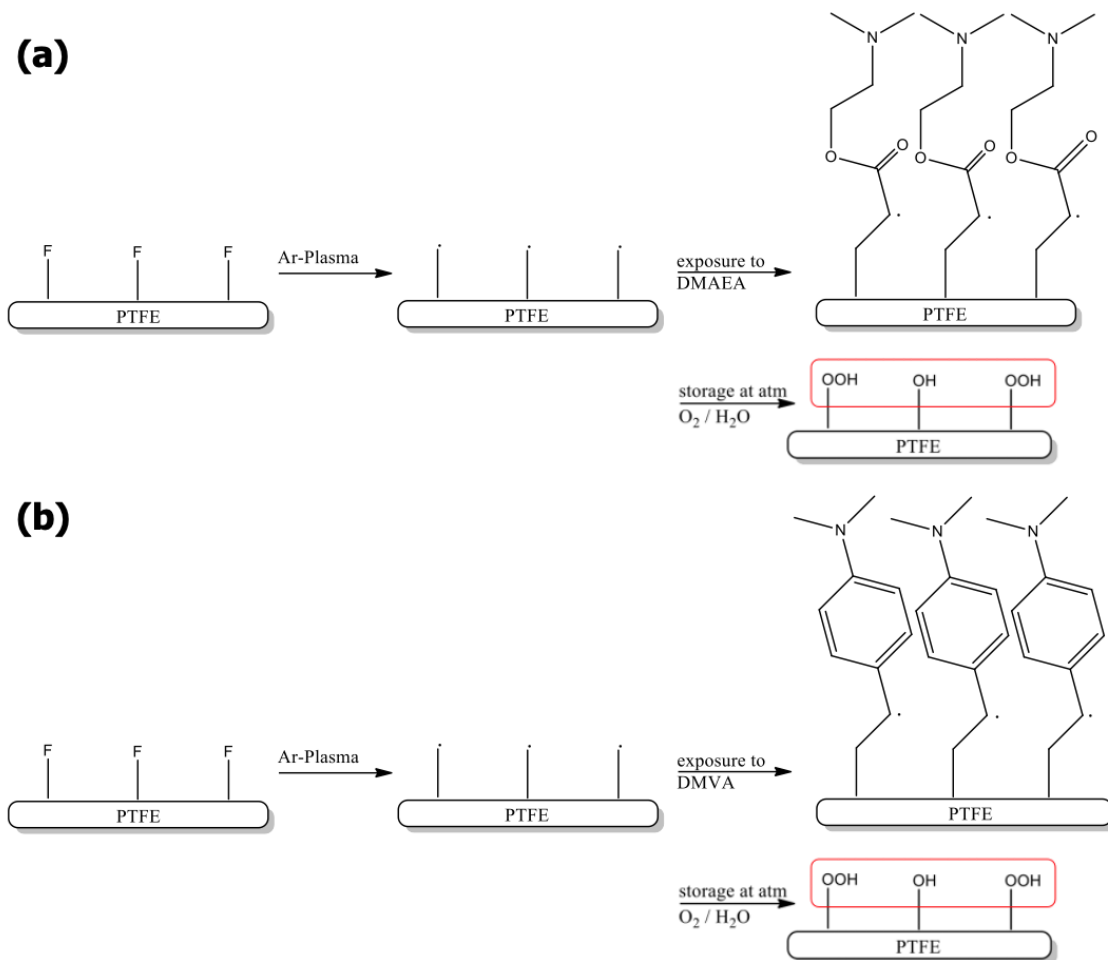


Figure 27: „grafting-from“ reaction mechanism of (a) DMAEA and (b) DMVA.

According to the XPS results in the following Table 11, no nitrogen was detected on the PTFE particle surface implying that neither DMAEA nor DMVA was grafted from the surface. In contrast, when the process was transferred to PTFE films, nitrogen was detected on the film surface confirming the successful grafting-from reaction of DMAEA or DMVA and the related introduction of N-functional groups to the PTFE surface. Furthermore, the results of PTFE films indicate, that a longer treatment time does not correlate with a higher nitrogen content on the film surface. As Figure 26 above shows, also a higher nitrogen content on the substrate's surface can be expected for treatment with DMAEA due to its less bulky structure and therefore higher grafting density. The results in Table 11 further support this assumption as DMAEA leads to a higher nitrogen content than DMVA.

Table 11: XPS results of PTFE films and PTFE particles after Ar plasma (1000 W, varying treatment duration) and grafting of DMAEA/DMVA.

		[at.%]									
		F	O	C	N	Al	Cu	Mg	Ca	Na	Si
PTFE films	Ar, 10 min, DMAEA pure	42.0 ± 0.8	9.6 ± 0.1	39.5 ± 0.6	2.9 ± 0.1	4.9 ± 0.2	0.5 ± 0.0	0.4 ± 0.0	0.4 ± 0.1	-	-
	Ar, 60 min, DMAEA pure	46.9 ± 0.3	7.3 ± 0.0	40.5 ± 0.2	2.1 ± 0.0	2.4 ± 0.3	0.2 ± 0.0	-	-	-	0.6 ± 0.2
	Ar, 10 min, DMVA pure	51.9 ± 0.6	5.3 ± 0,1	38.2 ± 0.7	1.2 ± 0.2	2.8 ± 0.1	0.4 *	-	-	0.8 *	-
PTFE particles	Ar, 10 min, DMAEA pure	69.6 ± 0.6	0.6 *	30.1 ± 0.2	-	-	-	-	-	-	-
	Ar, 10 min, DMAEA sol.	67.5 ± 1.1	0.4 *	32.3 ± 1.4	-	-	-	-	-	-	-
	Ar, 20 min, DMAEA sol.	67.1 ± 0.6	0.7 ± 0.2	32.3 ± 0.4	-	-	-	-	-	-	-
	Ar, 10 min, DMVA sol.	68.3 ± 0.5	-	31.7 ± 0.5	-	-	-	-	-	-	-

The following Figure 28 shows the representative XPS spectra of the PTFE film treated with Ar plasma for 10 minutes followed by pure DMAEA for 35 minutes.

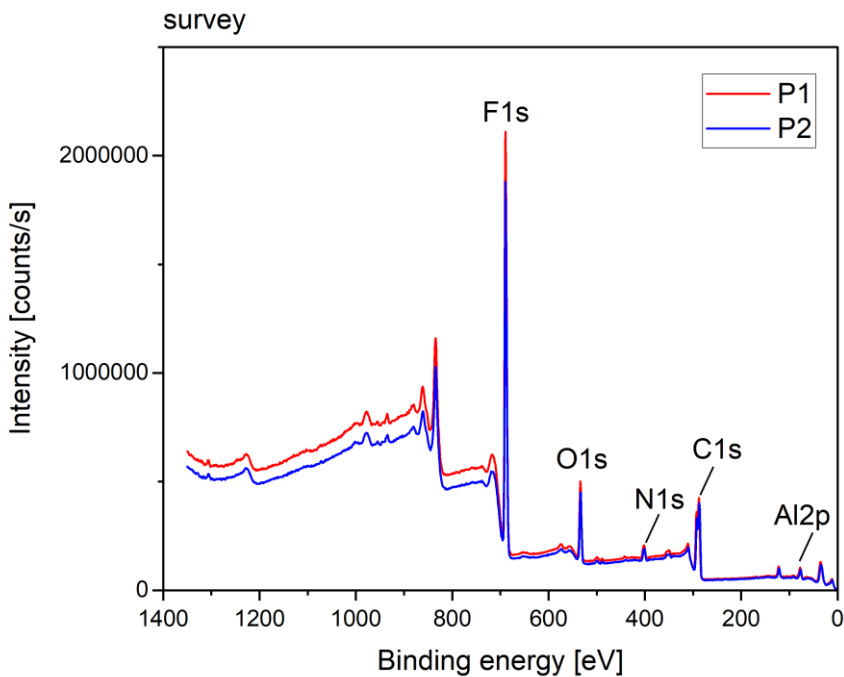


Figure 28: XPS spectra of the PTFE film after Ar plasma (1000 W, 10 min) and pure DMAEA.

Surface modification via NH₃ plasma

According to Wilson et al. [46], the use of NH₃ plasma results in a higher degree of surface defluorination than achieved with O₂ plasma. The NH₃ treatment leads to the formation of nitrogen- as well as oxygen-containing groups on the PTFE surface, as shown in the following Figure 29 [47].

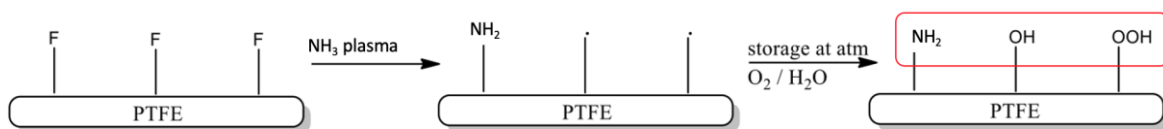


Figure 29: PTFE functionalisation via NH₃ plasma.

The following Table 12 shows the results for the PTFE particles after NH₃ plasma treatment and storage in either air or ethanol absolute. According to the results, NH₂ groups were successfully introduced to the particle surface at 1000 watts power. Interestingly, a shorter treatment duration leads to a higher nitrogen content of 0.9 ± 0.3 at.% and therefore more NH₂ groups on the surface. This may be explained by the fact that too long plasma treatment is often correlated with ablation, thus removing again the surface functional groups introduced before [33]. Besides nitrogen,

also some oxygen was detected. The presence of oxygen is consistent with the assumption of the reaction of free radicals with air molecules after the plasma treatment. Surprisingly, a higher nitrogen content was detected for samples stored in air. However, at the higher power setting of 3000 watts no nitrogen was detected on the plasma treated particle surface independent of the storage. Again, this may be related to excessive plasma treatment and the so-induced removal of the nitrogen containing moieties from the surface [33].

Table 12: XPS results of PTFE particles after NH₃ plasma (varying power, treatment duration and storage conditions).

Parameters	F [at.%]	O [at.%]	C [at.%]	N [at.%]
NH₃, 1000 W, 1 h, air	66.9 ± 0.9	0.4 ± 0.1	31.8 ± 0.8	0.9 ± 0.3
NH₃, 1000 W, 3 h, air	64.7 ± 5.1	0.6 *	34.5 ± 4.6	0.6 ± 0.1
NH₃, 3000 W, 1 h, air	68.1 ± 0.6	-	32.0 ± 0.6	-
NH₃, 1000 W, 1 h, ethanol	67.6 ± 1.9	0.4 *	31.8 ± 1.8	0.5 ± 0.2
NH₃, 1000 W, 3 h, ethanol	68.5 ± 0.2	-	31.4 ± 0.4	0.4 *
NH₃, 3000 W, 1 h, ethanol	67.8 ± 0.0	-	32.2 ± 0.0	-

The following Figure 30 shows the XPS spectra of the PTFE particles treated with NH₃ plasma at a plasma power of 1000 watts for 1 hour followed by storage in air versus the reference measurement of the untreated particles.

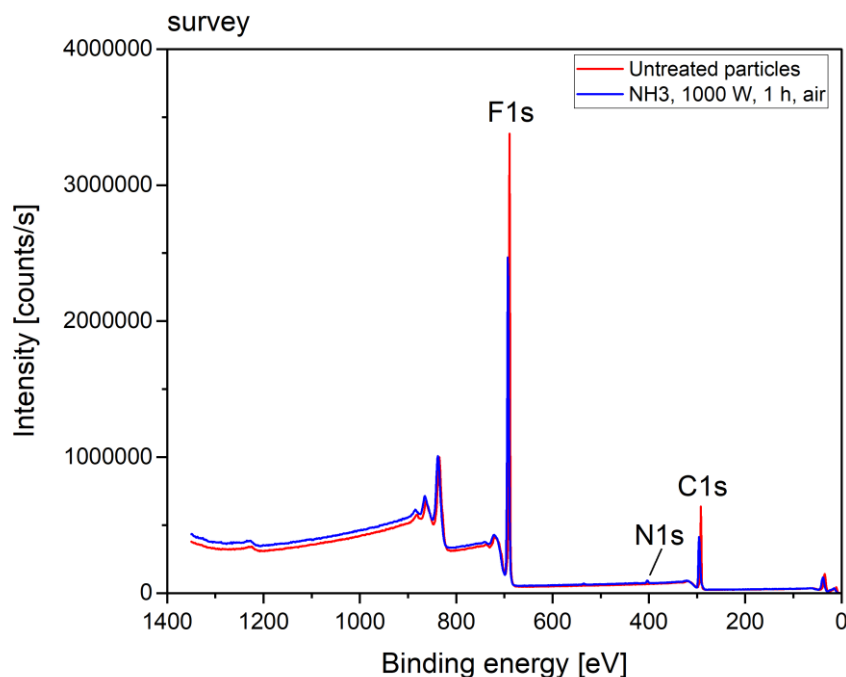


Figure 30: XPS spectra of the PTFE particles after NH₃ plasma (1000 W, 1 h, air) vs. the reference measurement.

Quaternisation

Due to the inhomogeneous nitrogen distribution across the PTFE particle surface after the H₂ plasma and APTES treatment, as indicated by the rather high standard deviation of the nitrogen content in Table 10, the quaternisation of amino groups was only conducted on samples treated with NH₃ plasma at 1000 watts power for 1 hour and 3 hours stored in air. As described in section 3.2, the particles were dispersed in a solution containing methanol, tributylamine and methyl iodide and were either left to rest or stirred for six hours to quaternise the amino moieties on the PTFE surface according to the following Figure 31.

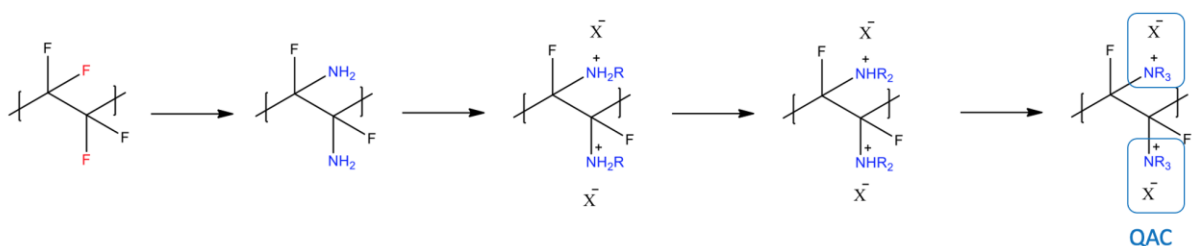


Figure 31: Introduction of amino groups and stepwise quaternisation of PTFE.

According to the XPS results in the following Table 13, the amino groups on the particle surface, which resulted from NH_3 plasma treatment (see Table 12) were not successfully converted to QACs since no nitrogen was detected after the quaternisation treatment anymore. A possible reason for this may be that the quaternisation lead to extensive generation of salts on the surface, which are soluble and thus removed from the surface in the purification steps. Therefore, the introduction of stable superficial QAC-moieties to PTFE particles was not yet successful and remains to be further developed beyond this thesis in order to achieve the desired ion conductivity of the binder material.

Table 13: XPS results of PTFE particles treated with NH_3 plasma after the quaternisation (non-stirred (ns) vs. stirred (s)).

Parameters	F [at.%]	O [at.%]	C [at.%]	N [at.%]
NH_3 , 1000 W, 1 h, air, ns	68.2 ± 0.5	-	31.8 ± 0.5	-
NH_3 , 1000 W, 3 h, air, ns	68.5 ± 0.1	-	31.5 ± 0.1	-
NH_3 , 1000 W, 1 h, air, s	68.1 ± 0.6	-	31.9 ± 0.6	-
NH_3 , 1000 W, 3 h, air, s	68.1 ± 0.8	-	31.9 ± 0.8	-

The following Figure 32 shows the XPS survey spectra of unmodified PTFE particles (reference), of PTFE particles after NH_3 plasma (NH_3 , 1000 W, 1 h, air) and the PTFE particles after the subsequent quaternisation (NH_3 , 1000 W, 1 h, air, ns). The close-up of the N1s peak in Figure 32 illustrates that amino groups were successfully introduced to the particle surface after NH_3 plasma. However, the absence of the N1s peak after the quaternisation reveals that this modification route was not successful.

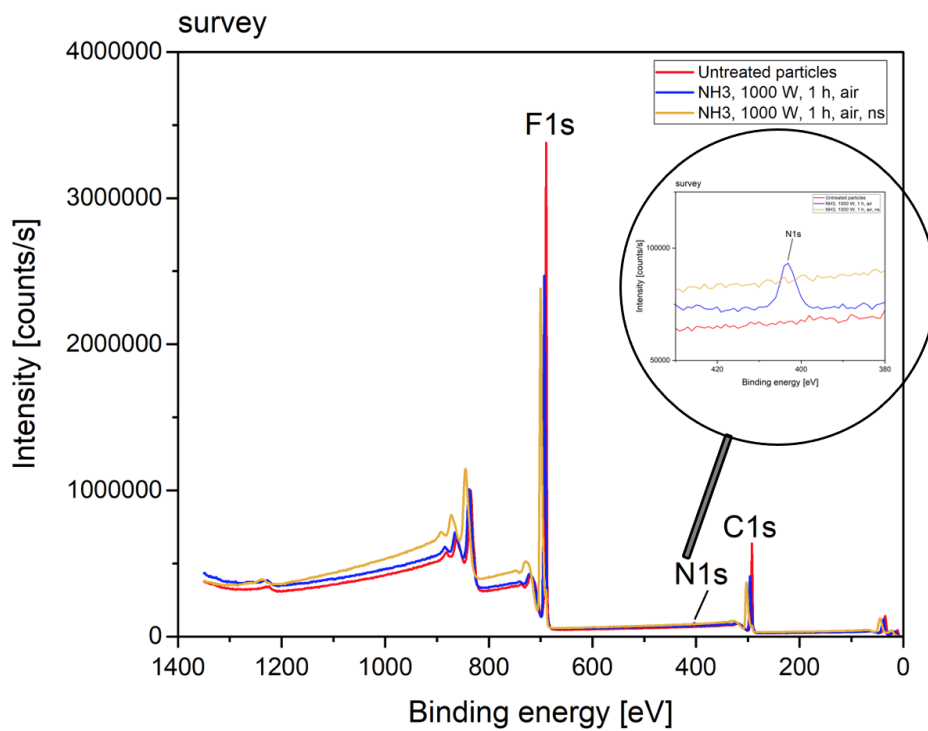


Figure 32: XPS spectra of unmodified PTFE particles (reference), the PTFE particles after NH₃ plasma (1000 W, 1 h, air) and the PTFE particles after the quaternisation.

5 Conclusion and outlook

The aim of this master's thesis was to functionalise PTFE particles towards increased surface polarity and ion conductivity for the use as a binder material in AEM water electrolysis cells. Hereby, the functionalisation process was divided into the following steps: the surface activation, the introduction of amino groups to the surface and the quaternisation of these amino groups. In order to evaluate the sub-steps and verify the functionalisation, the surface of the PTFE particles was examined using XPS to quantitatively determine the surface composition. Within the scope of this thesis, O₂, Ar and H₂ plasma were used for the purpose of activation. In principle, APTES can be coupled to the plasma-treated PTFE substrates to introduce amino groups to the surface. However, the XPS results show that O₂ and Ar plasma and subsequent APTES treatment did not introduce nitrogen moieties to the PTFE particle surface. As, according to the findings of Wilson et al. [46], the defluorination efficiency of Ar plasma is higher in comparison to O₂ plasma, "grafting-from" reactions of DMAEA and DMVA were conducted on PTFE films and particles after the Ar plasma alternatively. Although DMAEA and DMVA were successfully grafted from PTFE film surfaces, no nitrogen was detected on PTFE particle surfaces after the "grafting-from" reactions neither. Of the non-nitrogen containing plasmas, only the application of H₂ plasma and subsequent APTES treatment resulted in the incorporation of nitrogen into the PTFE particle surface (1.2 ± 0.7 at.%). Furthermore, treatment with NH₃ plasma was investigated for the modification of PTFE particles. Indeed nitrogen was detected on the particle surface after the NH₃ plasma treatment (0.9 ± 0.3 at.%). However, these nitrogen-containing functional groups were removed by the quaternisation reaction and subsequent purification. The transferability of the PTFE functionalisation from films to particles proved to be more challenging than anticipated and the objective of introducing ion conductivity through the quaternisation of the particles was not achieved within the scope of this master's thesis. However, suitable methods for the functionalisation of PTFE particles were identified, which will be the subject of further research work and development in the future. Therefore, the forthcoming phase of the project will concentrate on optimising the surface treatment of PTFE particles via plasma-based methods. Once the nitrogen content on the PTFE particle surface has been further

increased, the subsequent objective is to transfer the quaternisation process to particles to render the surface ionically conductive.

6 List of figures

Figure 1: Fundamental design of a water electrolysis cell [12].	3
Figure 2: Water electrolysis cell designs: a.) conventional and b.) zero-gap [13].	3
Figure 3: AWE cell structure [16].	6
Figure 4: PEM cell structure [18].	7
Figure 5: SOE cell structure [16].	9
Figure 6: AEM cell structure [24].	11
Figure 7: Structural formula of PTFE.	14
Figure 8: Mechanism of radical-initiated homopolymerisation of [30].	14
Figure 9: Schematic setup of a low-pressure plasma system [36].	17
Figure 10: QAC reaction possibilities: (a) elimination, (b) substitution, (c) rearrangement and (d) ion exchange reactions [40].	20
Figure 11: Quaternisation of (a) primary, (b) secondary and (c) tertiary amines [40].	20
Figure 12: General structure of an XPS measuring device [43].	22
Figure 13: X-ray induced emission of an (a) XPS electron and (b) Auger electron [43].	24
Figure 14: Exemplary XPS-spectrum [43].	25
Figure 15: Strategic flow chart for the PTFE particle functionalisation.	30
Figure 16: Folded Kapton® tape strips inside a screw cap bottle.	31
Figure 17: PTFE functionalisation via O ₂ plasma.	35
Figure 18: Two-step coupling of APTES to PTFE surfaces.	36
Figure 19: PTFE functionalisation via Ar plasma.	38
Figure 20: XPS spectra of the PTFE film after O ₂ or Ar plasma (1000 W, 10 min) and subsequent modification with APTES and the reference measurement.	40
Figure 21: XPS spectra of the PTFE film after O ₂ plasma (1000 W, 10 min) and subsequent modification with APTES.	42
Figure 22: XPS spectra of the PTFE film after Ar plasma (1000 W, 10 min) and subsequent modification with APTES.	43
Figure 23: XPS spectra of SiO ₂ particles after O ₂ plasma (1000 W, 10 min) and modification with APTES.	44
Figure 24: PTFE functionalisation via H ₂ plasma.	44

Figure 25: XPS spectra of the PTFE film after H ₂ plasma (1000 W, 10 min) and subsequent modification with APTES vs. the reference measurement.	45
Figure 26: Structural formula of (a) DMAEA [48] and (b) DMVA [49].	46
Figure 27: „grafting-from“ reaction mechanism of (a) DMAEA and (b) DMVA.	47
Figure 28: XPS spectra of the PTFE film after Ar plasma (1000 W, 10 min) and pure DMAEA.	49
Figure 29: PTFE functionalisation via NH ₃ plasma.	49
Figure 30: XPS spectra of the PTFE particles after NH ₃ plasma (1000 W, 1 h, air) vs. the reference measurement.	51
Figure 31: Introduction of amino groups and stepwise quaternisation of PTFE.	52
Figure 32: XPS spectra of unmodified PTFE particles (reference), the PTFE particles after NH ₃ plasma (1000 W, 1 h, air) and the PTFE particles after the quaternisation.	53

7 List of tables

Table 1: List of used chemicals.	26
Table 2: List of materials used in the experiments.....	27
Table 3: List of used devices.....	28
Table 4: O ₂ , Ar or H ₂ plasma treatment durations.	31
Table 5: NH ₃ plasma power and treatment durations.	33
Table 6: XPS results of PTFE particles directly after O ₂ plasma and after O ₂ plasma and subsequent modification with APTES.....	37
Table 7: XPS results of PTFE particles directly after Ar plasma and after Ar plasma and subsequent modification with APTES.....	39
Table 8: XPS results of PTFE films after O ₂ or Ar plasma and APTES before/after cleaning in ethanol absolute.....	41
Table 9: XPS results of SiO ₂ particles after O ₂ plasma (1000 W, 10 min) and subsequent modification with APTES.	43
Table 10: XPS results of PTFE particles after H ₂ plasma (1000 W, 10 min) and subsequent modification with APTES.	45
Table 11: XPS results of PTFE films and PTFE particles after Ar plasma (1000 W, varying treatment duration) and grafting of DMAEA/DMVA.	48
Table 12: XPS results of PTFE particles after NH ₃ plasma (varying power, treatment duration and storage conditions).	50
Table 13: XPS results of PTFE particles treated with NH ₃ plasma after the quaternisation (non-stirred (ns) vs. stirred (s)).....	52
Table 14: Declaration of AI-based tools used in this thesis.	64

8 Bibliography

- [1] G. Primc, "Recent advances in surface activation of polytetrafluoroethylene (PTFE) by gaseous plasma treatments," Oct. 01, 2020, *MDPI AG*. doi: 10.3390/polym12102295.
- [2] A. Ursúa, L. M. Gandía, and P. Sanchis, "Hydrogen Production from Water Electrolysis: Current Status and Future Trends," 2011. Accessed: Feb. 13, 2023. [Online]. Available: <https://ieeexplore.ieee.org/document/5898382>
- [3] A. Midilli, I. Dincer, and M. Ay, "Green energy strategies for sustainable development," *Energy Policy*, vol. 34, no. 18, pp. 3623–3633, Dec. 2006, doi: 10.1016/j.enpol.2005.08.003.
- [4] "Energy Security – Topics - IEA." Accessed: Aug. 08, 2024. [Online]. Available: <https://www.iea.org/topics/energy-security>
- [5] H. A. Miller *et al.*, "Green hydrogen from anion exchange membrane water electrolysis: A review of recent developments in critical materials and operating conditions," May 01, 2020, *Royal Society of Chemistry*. doi: 10.1039/c9se01240k.
- [6] "Alternative Fuels Data Center: Hydrogen Basics." Accessed: Aug. 08, 2024. [Online]. Available: <https://afdc.energy.gov/fuels/hydrogen-basics>
- [7] S. A. Grigoriev, V. N. Fateev, D. G. Bessarabov, and P. Millet, "Current status, research trends, and challenges in water electrolysis science and technology," *Int J Hydrogen Energy*, vol. 45, no. 49, pp. 26036–26058, Oct. 2020, doi: 10.1016/j.ijhydene.2020.03.109.
- [8] C. E. Mortimer and U. Müller, *Basiswissen der Chemie*, 12th ed. Thieme Gruppe, 2015.
- [9] Z. Ahmad, *Principles of corrosion engineering and corrosion control*. Elsevier/BH, 2006.
- [10] F. Han *et al.*, "High electronic conductivity as the origin of lithium dendrite formation within solid electrolytes," *Nat Energy*, vol. 4, no. 3, pp. 187–196, Mar. 2019, doi: 10.1038/s41560-018-0312-z.
- [11] V. S. (Vladimir S. Bagotskiĭ, *Fundamentals of electrochemistry*. Wiley-Interscience, 2006.

-
- [12] M. M. Rashid, M. K. Al Mesfer, H. Naseem, and M. Danish, "Hydrogen Production by Water Electrolysis: A Review of Alkaline Water Electrolysis, PEM Water Electrolysis and High Temperature Water Electrolysis," 2015. [Online]. Available: <https://www.researchgate.net/publication/273125977>
- [13] J. Brauns and T. Turek, "Alkaline water electrolysis powered by renewable energy: A review," Feb. 01, 2020, *MDPI AG*. doi: 10.3390/pr8020248.
- [14] P. Millet and S. Grigoriev, "Water Electrolysis Technologies," in *Renewable Hydrogen Technologies: Production, Purification, Storage, Applications and Safety*, Elsevier B.V., 2013, pp. 19–41. doi: 10.1016/B978-0-444-56352-1.00002-7.
- [15] Z. Zakaria and S. K. Kamarudin, "A review of alkaline solid polymer membrane in the application of AEM electrolyzer: Materials and characterization," Oct. 25, 2021, *John Wiley and Sons Ltd*. doi: 10.1002/er.6983.
- [16] F. M. Sapountzi, J. M. Gracia, C. J. Weststrate, H. O. A. Fredriksson, and J. W. Niemantsverdriet, "Electrocatalysts for the generation of hydrogen, oxygen and synthesis gas," Jan. 01, 2017, *Elsevier Ltd*. doi: 10.1016/j.pecs.2016.09.001.
- [17] Q. Xu *et al.*, "Anion Exchange Membrane Water Electrolyzer: Electrode Design, Lab-Scaled Testing System and Performance Evaluation," Sep. 01, 2022, *Elsevier B.V.* doi: 10.1016/j.enchem.2022.100087.
- [18] H. Ito, T. Maeda, A. Nakano, A. Kato, and T. Yoshida, "Influence of pore structural properties of current collectors on the performance of proton exchange membrane electrolyzer," *Electrochim Acta*, vol. 100, pp. 242–248, Jun. 2013, doi: 10.1016/j.electacta.2012.05.068.
- [19] "PEM electrolysis." Accessed: Sep. 20, 2023. [Online]. Available: <https://matthey.com/products-and-markets/pgms-and-circularity/pgm-chemicals-and-catalysts/pem-electrolysis>
- [20] A. M. Osborn and R. B. Moore, "Morphology of Proton Exchange Membranes," in *Polymer Science: a Comprehensive Reference: Volume 1-10*, vol. 1–10, Elsevier, 2012, pp. 721–766. doi: 10.1016/B978-0-444-53349-4.00288-0.
- [21] M. Carmo, D. L. Fritz, J. Mergel, and D. Stolten, "A comprehensive review on PEM water electrolysis," Apr. 22, 2013. doi: 10.1016/j.ijhydene.2013.01.151.
- [22] "What Are the Platinum Group Metals? — Reclaim, Recycle, and Sell your Precious Metal Scrap." Accessed: Dec. 22, 2023. [Online]. Available:

-
- <https://www.specialtymetals.com/blog/2015/3/25/what-are-the-platinum-group-metals>
- [23] S. Shiva Kumar and H. Lim, "An overview of water electrolysis technologies for green hydrogen production," Nov. 01, 2022, *Elsevier Ltd.* doi: 10.1016/j.egy.2022.10.127.
- [24] J. Yang *et al.*, "Non-precious electrocatalysts for oxygen evolution reaction in anion exchange membrane water electrolysis: A mini review," Oct. 01, 2021, *Elsevier Inc.* doi: 10.1016/j.elecom.2021.107118.
- [25] S. Oikonomidis, M. Ramdin, O. A. Moulto, A. Bos, T. J. H. Vlught, and A. Rahbari, "Transient modelling of a multi-cell alkaline electrolyzer for gas crossover and safe system operation," *Int J Hydrogen Energy*, vol. 48, no. 88, pp. 34210–34228, Oct. 2023, doi: 10.1016/j.ijhydene.2023.05.184.
- [26] "Roy J. Plunkett | Science History Institute." Accessed: Feb. 14, 2024. [Online]. Available: <https://www.sciencehistory.org/education/scientific-biographies/roy-j-plunkett/>
- [27] S. Ebnesajjad, "History of Polytetrafluoroethylene and Expanded PTFE Membrane," in *Expanded PTFE Applications Handbook*, Elsevier, 2017, pp. 1–7. doi: 10.1016/b978-1-4377-7855-7.00001-8.
- [28] S. Ebnesajjad, "Manufacturing Polytetrafluoroethylene," in *Introduction to Fluoropolymers - Materials, Technology and Applications*, Elsevier, 2013, pp. 91–124. doi: 10.1016/b978-1-4557-7442-5.00007-3.
- [29] G. J. Puts, P. Crouse, and B. M. Ameduri, "Polytetrafluoroethylene: Synthesis and Characterization of the Original Extreme Polymer."
- [30] A. Xu *et al.*, "Radical homopolymerization of tetrafluoroethylene initiated by perfluorodiacyl peroxide in supercritical carbon dioxide: Reaction mechanism and initiation kinetics," *Eur Polym J*, vol. 48, no. 8, pp. 1431–1438, Aug. 2012, doi: 10.1016/j.eurpolymj.2012.05.012.
- [31] D. O'hagan, "Understanding organofluorine chemistry. An introduction to the C–F bond," *Chem Soc Rev*, vol. 37, no. 2, pp. 308–319, Jan. 2008, doi: 10.1039/b711844a.
- [32] Wolfgang Kaiser, "Kunststoffchemie für Ingenieure," 2011. [Online]. Available: www.hanser-elibrary.com

-
- [33] A. J. Kinloch, *Adhesion and Adhesives*. Dordrecht: Springer Netherlands, 1987. doi: 10.1007/978-94-015-7764-9.
- [34] G. Habenicht, *Kleben*. Springer Berlin Heidelberg, 2009. doi: 10.1007/978-3-540-85266-7.
- [35] L. Bárdos and H. Baránková, "Plasma processes at atmospheric and low pressures," *Vacuum*, vol. 83, no. 3, pp. 522–527, Oct. 2008, doi: 10.1016/j.vacuum.2008.04.063.
- [36] "Low-pressure plasma: Cleaning, activation, coating, etching - Plasma.com." Accessed: Sep. 25, 2024. [Online]. Available: <https://www.plasma.com/en/low-pressureplasma/>
- [37] U. Vohrer, "Interfacial engineering of functional textiles for biomedical applications," in *Plasma Technologies for Textiles: A Volume in Woodhead Publishing Series in Textiles*, Elsevier Ltd, 2007, pp. 202–227. doi: 10.1533/9781845692575.2.202.
- [38] K. S. Johansson, "Surface Modification of Plastics," in *Applied Plastics Engineering Handbook: Processing, Materials, and Applications: Second Edition*, Elsevier Inc., 2017, pp. 443–487. doi: 10.1016/B978-0-323-39040-8.00020-1.
- [39] G. Primc and M. Mozetič, "Hydrophobic Recovery of Plasma-Hydrophilized Polyethylene Terephthalate Polymers," 2022, doi: 10.3390/polym14122496.
- [40] F. Bureš, "Quaternary Ammonium Compounds: Simple in Structure, Complex in Application," Jun. 01, 2019, *Springer International Publishing*. doi: 10.1007/s41061-019-0239-2.
- [41] H. Z. Sommer, I. Lipp, and L. L. Jackson, "Alkylation of Amines. A General Exhaustive Alkylation Method for the Synthesis of Quaternary Ammonium Compounds," 1971.
- [42] R. J. T. Kleijwegt, S. Y. Doruiter, W. Winkenwerder, and J. van der Schaaf, "Investigating tertiary amine alkylation/benzylation kinetics with ramp-flow in a plug-flow reactor using in-line ¹H NMR spectroscopy," *Chemical Engineering Research and Design*, vol. 168, pp. 317–326, Apr. 2021, doi: 10.1016/j.cherd.2021.02.021.
- [43] F. A. Stevie and C. L. Donley, "Introduction to x-ray photoelectron spectroscopy," *Journal of Vacuum Science & Technology A: Vacuum, Surfaces, and Films*, vol. 38, no. 6, Dec. 2020, doi: 10.1116/6.0000412.

-
- [44] G. Lukowski and E. M. Arndt, "Röntgen-Photoelektronenspektroskopie."
- [45] H. Hunke *et al.*, "Low-pressure H₂, NH₃ microwave plasma treatment of Polytetrafluoroethylene (PTFE) powders: Chemical, thermal and wettability analysis," *Materials*, vol. 8, no. 5, pp. 2258–2275, 2015, doi: 10.3390/ma8052258.
- [46] D. J. Wilson, R. L. Williams, and R. C. Pond, "Plasma modification of PTFE surfaces - Part I: Surfaces immediately following plasma treatment," *Surface and Interface Analysis*, vol. 31, no. 5, pp. 385–396, 2001, doi: 10.1002/sia.1065.
- [47] J. P. Badey, E. Espuche, Y. Jugnett, B. Chabert, and T. M. Due, "Influence of chemical and plasma treatments the adhesive properties of PTFE with an epoxy resin," 1996.
- [48] "2-(Dimethylamino)ethylacrylat contains <2,000 ppm MEHQ as inhibitor, 98% | Sigma-Aldrich." Accessed: Sep. 29, 2024. [Online]. Available: <https://www.sigmaaldrich.com/AT/de/product/aldrich/330957?srsId=AfmBOoqga3u3rwYQJQtXZQn3RfLrLDlzS0CAq0b-fu2vbvcgIpCxb1K6>
- [49] "AB451271 | CAS 2039-80-7 – abcr Gute Chemie." Accessed: Sep. 29, 2024. [Online]. Available: https://abcr.com/de_de/ab451271

9 Appendix

9.1 AI declaration

The use of AI-based tools in this thesis is declared in the following Table 14.

Table 14: Declaration of AI-based tools used in this thesis.

Subject	Percentage of AI (in %)	Tool / Version	Note	Link to prompting
Translating	20	DeepL Translator (web version)	n/a	n/a
Improvement of readability	10	DeepL Write (web version)	n/a	n/a